

UNCLASSIFIED

AD **409 168**

DEFENSE DOCUMENTATION CENTER

FOR

SCIENTIFIC AND TECHNICAL INFORMATION

CAMERON STATION, ALEXANDRIA, VIRGINIA



UNCLASSIFIED

NOTICE: When government or other drawings, specifications or other data are used for any purpose other than in connection with a definitely related government procurement operation, the U. S. Government thereby incurs no responsibility, nor any obligation whatsoever; and the fact that the Government may have formulated, furnished, or in any way supplied the said drawings, specifications, or other data is not to be regarded by implication or otherwise as in any manner licensing the holder or any other person or corporation, or conveying any rights or permission to manufacture, use or sell any patented invention that may in any way be related thereto.

This Document
Reproduced From
Best Available Copy

Report No. 1

409 168

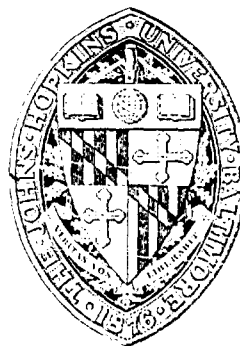
Contract DA-36-039-SC-89147
File No. 1033-PM-62-93-93(4102)

CATALOGED BY DDC
AS AD No. 409168

Sponsored by
U. S. Army Electronics Research and Development Laboratory
Ft. Monmouth, New Jersey

DIELECTRICS FOR SATELLITES AND SPACE VEHICLES

Final Report for the period
March 1, 1962 to March 31, 1963



DIELECTRICS LABORATORY
The Johns Hopkins University
Baltimore, Maryland

ASTIA Availability Notice

Qualified requestors may
obtain copies from ASTIA

Report No. 1
April 30, 1963

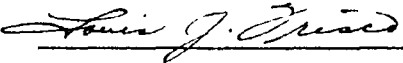
Contract DA-36-039-SC-89147
File No. 1033-PM-67-93-93(4102)

DIELECTRICS FOR SATELLITES
AND SPACE VEHICLES

Final Report
for the period
March 1, 1962 to March 31, 1963

Prepared by:
Louis J. Frisco
A.M. Muhlbaum
Edward A. Szymkowiak

Approved by:



Louis J. Frisco
Research Contract Director

THE JOHNS HOPKINS UNIVERSITY
DIELECTRICS LABORATORY
405 NORTH CAROLINE STREET
BALTIMORE 31, MARYLAND

CONTENTS

I.	Purpose	1
	A. Objective	1
	B. Materials	1
	C. Electrical Properties	2
	D. Environmental Conditions	2
II.	Abstract	3
III.	Factual Data	5
	A. Facilities	5
	1. Laboratory Relocation	5
	2. Environmental Chambers	5
	3. Loss-Specimen Holder	5
	B. Electrical Breakdown in High Vacuum	7
	1. Purpose	7
	2. Background	7
	3. Experimental Method	10
	4. Results and Conclusions	12
	C. X-Ray Induced Conductivity	12
	1. Experimental Procedure	12
	2. Experimental Results	15
	3. Discussion of Results	19
	D. X-Ray Induced A-C Losses	22
	1. Previous Results	22
	2. Experimental Results	23
	3. Discussion of Results	26
	E. Electric Strength Measurements	27
IV.	Conclusions	31
V.	Recommendations	33
VI.	Cited References	35
VII.	Identification of Personnel	37

CONTENTS

VIII. Identification of Personnel	37
IX. Tables	41
X. Illustrations	51
Appendix I - Summary of Tests on Multiconductor Cable Connectors	73
Appendix II - Summary of Electrical Data on Siloxane Dielectric Compositions for Antenna Mount Insulators	87
Appendix III - Dielectric Properties of Extraterrestrial Dust	97

I. Purpose.

A. Objective. This program is an extension of the study of simulated high altitude and outer space environments on the electrical properties of electrical insulating materials that was initiated under Contract DA-36-039-SC-78321 (March 1, 1959 - February 28, 1962). The objective of this program is to provide a better understanding of the behavior of electrical insulating materials in a space environment.

B. Materials. In the previous program, data was obtained on 21 materials. The materials of that group that are referred to in this report are identified as follows:

<u>Designation</u>	<u>Description and Supplier</u>
TFE-6	Polytetrafluoroethylene extrusion resin, commercial designation TFE-6. E.I. du Pont de Nemours and Company, Wilmington, Delaware.
TFE-7	Polytetrafluoroethylene molding resin, commercial designation TFE-7. E.I. du Pont de Nemours and Company, Wilmington, Delaware.
FEP-100	Copolymer of tetrafluoroethylene and hexafluoropropylene, melt processable resin, commercial designation FEP-100. E.I. du Pont de Nemours and Company, Wilmington, Delaware.
Mylar 130-100T	Polyester film, commercial designation MYLAR 130-100T, highly oriented in the long, or machine direction. E.I. du Pont de Nemours and Company, Circleville, Ohio.
Mylar 130-100A	Polyester film, commercial designation MYLAR 130-100-A, same composition as 130-100T but not as highly oriented.
Mylar 130-100C	Polyester, capacitor film, commercial designation MYLAR 130-100C. E.I. du Pont de Nemours and Company, Circleville, Ohio.

PURPOSE

One additional material was included in the study of the effects of x-ray irradiation on a-c loss properties. It is identified as follows:

C-1147	Composition of methyl styrene with a small amount of dimethyl siloxane additive. Specimens supplied by the Delaware Research and Development Corporation, Wilmington, Delaware.
--------	---

C. Electrical Properties.

1. Dielectric constant at 60 cps, 2, 18 and 100 Mc.
2. Dissipation factor at 60 cps, 2, 18 and 100 Mc.
3. Volume resistivity, d-c.
4. Surface resistivity, d-c.
5. Electric strength 60 cps, 2, 18 and 100 Mc.
6. Flashover strength 60 cps, 2, 18 and 100 Mc.
7. Microwave transmission properties at frequencies up to 10 Gc as time and facilities permitted.

D. Environmental Conditions.

1. Temperatures of -55, 25, 85 and 125C.
2. Minimum vacuum of 10^{-4} torr.
3. Solar x-rays.
4. Solar ultraviolet.
5. Chemisphere and ionosphere conditions.

II. Abstract

Further results of a study of simulated space environment on the electrical properties of solid dielectric materials are reported.

High-vacuum sparkover measurements in the presence of a strong magnetic field show that the breakdown voltage does not depend on effects produced by primary electrons striking the anode.

Preliminary results indicate that x-ray induced conductivity, σ_x , in Mylar-C, TFE-7 and polyethylene was voltage dependent, following the relationship $\log \sigma_m \sim V$. At a fixed voltage, σ_m was proportional to R^Δ , where R is the dose rate and Δ is a constant. The time required for σ_x to reach a maximum value was not proportional to $R^{-\mu}$, where R is the dose rate and μ is a constant, as reported elsewhere in the literature. With Mylar-C, σ_x is temperature dependent, showing a complex behavior in the range of the second order transition temperature. Insufficient data does not permit final conclusions.

X-ray induced a-c losses in TFE resins (previously reported) are greatly influenced by the presence of oxygen during sintering. Diffusion (specimen thickness) plays a minor role in irradiation effects on a-c loss properties.

An improved specimen for electric strength measurements on solids, at frequencies up to 100 Mc, is described.

Some phases of the investigation will be continued under Contract NAS8-5253.

III. Factual Data.

A. Facilities.

1. Laboratory Relocation. During the present reporting period the Dielectrics Laboratory was moved from 1315 St. Paul Street, Baltimore, Maryland to 405 North Caroline Street, Baltimore, Maryland. Since it was necessary to dismantle the existing high-voltage test berths,* it was convenient to make design changes that would increase the versatility of existing equipment. In the new installation, high voltage tests at d-c, 60 cps, 1, 38 and 180 kc can be made in the same berth. All of these voltage sources and their accessories can be operating from a single control-console.

The radio-frequency test circuits that had previously been located in a walk-in shielded-room are now installed in a 2 1/2' x 4' x 8' shielded enclosure. Ready access to all parts of the enclosure is provided by removable panels and doors. This installation is used for high-voltage experiments in the 2 to 18 Mc range.

2. Environmental Chambers. The high-vacuum pumping systems and test cells that were used in this study have been fully described in previous reports. It is only necessary to mention here that the x-ray generator uses two Machlett AEG-50 beryllium window tubes that are capable of continuous operation at voltages up to 50 KV peak and anode currents up to 50 ma. The maximum output intensity of each tube is 1.60 milliwatts/cm² at a distance of 155 mm from the target.

3. Temperature Controlled Loss-Specimen Holder. A guarded specimen holder was designed to facilitate dielectric constant and dissipation factor measurements at frequencies up to 100 kc, over the temperature range of -50 to 125°C during x-ray irradiation in vacuum. Only preliminary measurements have been made, but the general construction is of interest.

The holder was designed to be mounted in an existing vacuum chamber, which has provisions for introducing x-ray irradiation. Therefore, it was not necessary for the holder itself to be vacuum sealed. Its only functions are: (a) to support the specimen and the electrodes, and (b) to provide a constant-temperature surface which surrounds the specimen. The electrode pattern is a common arrangement of a guarded electrode and a guard-ring on one side of a flat specimen and a single electrode on the other side.

The guarded electrode and the guard ring are mounted in the closed end of a cylindrical brass tube (4" diameter x 3 1/2" long). This cylinder is nested in a larger cylinder (4 1/2" diameter x 4" long) so that there is a spacing of about 1/4" between the inner and outer cylinders. Heater wires are wrapped around the outside of the inner cylinder and a cooling coil is wrapped around the outer cylinder, which can serve as a heat shield or a cooling surface, depending on the temperature of the experiment. The x-ray beam enters through an opening in a cover plate at the open end of the specimen holder.

The guarded electrode and the guard ring are insulated from the end-plate and rigidly fastened to insulated studs that serve as electrical terminals. A thin coating of silver, applied directly on the specimen, serves as the high-voltage electrode. Any additional metal in this location would shield the specimen from the x-ray beam. Electrical contact with the silver coating is made through a metal ring which is fixed in an insulated insert.

Using thermocouples for temperature measurement, and a thermistor in the temperature control circuit, the specimen temperature can be maintained constant within 0.1°C.

B. Electrical Breakdown in High-Vacuum.

1. Purpose. The results of a study of sparkover in high vacuum were discussed in the Final Report of Contract DA-36-039-SC-78321. In this previous study, flashover across the surface of an insulating material and sparkover between spherical electrodes were investigated. It was shown that the inherently high electric strength of air at pressures in the 10^{-6} torr range is compromised by cathode effects. The surface roughness of the cathode proved to be a critical factor. During the present reporting period, additional experiments were conducted for the purpose of determining if secondary effects at the anode contribute to the breakdown process.

2. Background. A comprehensive discussion of gaseous breakdown can be found in a recent book by F. Llewellyn-Jones⁽¹⁾. For the purposes of this discussion it is only necessary to make a few general remarks.

A self-sustained discharge occurs in a gas when each electron avalanche that crosses the breakdown gap causes (on the average) at least one secondary electron that gives rise to a new avalanche. At pressures where the mean free path of the electrons is short compared to the gap between the electrodes, the gas molecules in the gap play an important part in the breakdown mechanism. The electrons which collide with these gas molecules can produce photons or positive gas ions which, in turn, can generate enough secondary electrons for a self-sustained discharge. However, at lower pressures where the mean free path is much longer than the electrode spacing, as in laboratory experiments when the pressure is below 10^{-5} torr, the chance for a collision of an electron with a gas molecule is much smaller. Therefore, the residual gas molecules between the electrodes do not contribute to the breakdown mechanism in high-vacuum. Consequently, the effects originating at the electrodes must play a dominant role.

There are several ways in which the cathode and anode could contribute to the breakdown mechanism, other than creating the electric field between the electrodes. It is well established that the high fields located at sharp points on the cathode cause field emission of electrons. The electrons are accelerated by the electric field and bombard the anode (2, 3, 4, 5, 6, 7). The question arises: are there any secondary effects at the anode which, in turn, could generate secondary electrons to obtain a self-sustained discharge?

Many hypotheses have been offered concerning secondary effects at the anode caused by the bombardment by primary electrons (6, 7, 8, 11). These hypotheses are concerned with:

- (a) Release of positive gas or metal ions from the anode.
These ions, which are accelerated in the electric field, bombard the cathode and could release secondary electrons.
- (b) Formation of x-rays at the anode which in turn release secondary electrons at the cathode by photo-emission.
- (c) Local heating of the anode surface to a high temperature causing the liberation of large amounts of adsorbed gas and metal vapor which destroy the vacuum and cause a gaseous discharge to occur. Charged metal particles detached from the cathode could contribute to this effect by bombarding the anode (8, 10).
- (d) Release of charged metal particles from the anode bombarding the cathode and thereby causing effects as described in (c) above.

To test these hypotheses other workers have measured:

- (a) The average number of ions and x-ray quanta released from the anode per bombarding electron.
- (b) The average number of secondary electrons released from the cathode per ion or x-ray quantum impinging on the cathode.

The values obtained from these measurements were too low to account for any of the effects described above^(8, 9, 10). However, it is difficult to measure voltage-dependent secondary effects just before and during development of breakdown because of the large variation in breakdown voltage and the fact that breakdown develops in less than a microsecond.

Dyke, Trolan, et al^(3, 4, 5) have shown, by using a sharply pointed cathode and pulse voltages, that the bombardment of the cathode by positive ions from the anode is not essential for breakdown. The time in which breakdown occurs is less than the time required for an ion to traverse the gap between the electrodes. This is so much more the case for the heavier metal particles which are detached from the anode. They report that the large field-emission currents, at voltages near the breakdown voltage, heat the thin tip on the cathode. This causes thermo-emission which results in an increase in the total emission from the cathode. This runaway condition continues until the metal point evaporates and a gaseous discharge in the metal vapor occurs. The results of the following experiments not only support the statements of Dyke and Trolan, but show that none of the secondary effects at the anode are essential for breakdown. The only function of the anode in initiating breakdown is to create the electrical field at the cathode.

3. Experimental Method. The end of a 1/16" diameter copper wire was filed to a conical tip. The tip of the wire was used as the cathode opposite a flat brass anode, as shown in Figure 1. The distance between the tip of the cathode and the anode was about 3/8". Both electrodes were placed in a cylindrical glass cell which was evacuated by an oil diffusion pump. The pressure in the cell was held at about 10^{-5} torr. The prebreakdown current could be measured with the micromicroammeter, M. The cell was placed between the poles of an electromagnet, so that the magnetic field was perpendicular to the axis of the glass cylinder. Because the electric field is greatest at the tip of the needle, the field emission current will originate there. With no magnetic field, the electrons emerge from the tip, cross the gap in nearly straight lines, and impinge on the anode.

When the magnetic field is applied in the z-direction (see Figure 1) the electrons, which are moving in the x-direction, are deflected in the y-direction in accordance with the classical relationships:

$$F_x = eE = m \frac{d^2x}{dt^2},$$

$$F_y = Be \frac{dx}{dt} = m \frac{d^2y}{dt^2},$$

and
$$y = \frac{B}{3} \left(\frac{2d}{m} \right)^{1/2} E^{-1/2} x^{3/2},$$

where, F_x = x-component of the force on an electron

F_y = y-component of the force on an electron

B = magnetic field strength (z-direction)

E = electric field strength (x-direction)

e = electronic charge

m = electronic mass

t = time

y = deflection of electron in y -direction

Near the tip of the cathode, where the electrons have a low velocity, the force, F_y , and the displacement, y , are small. Therefore, the presence of the magnetic field has little effect on the primary electrons near the cathode. However, with a strong enough magnetic field the electrons can be deflected far enough to completely miss the anode. Any secondary effects associated with the anode would then be drastically changed as the magnetic field is switched on and off. Therefore, if the breakdown voltage is not affected by the presence of the magnetic field, the mechanism that initiates breakdown is not dependent on secondary effects at the anode. The essential secondary effects must then be occurring at the cathode only.

Because the inherent spread in results for vacuum breakdown measurements is large enough to mask effects that would be significant, the following step-by-step procedure was used in studying the influence of the magnetic field on the breakdown voltage:

The direct voltage was increased in steps of 300 volts, a value considerably smaller than the normal spread in results. In one series of tests, the magnetic field was introduced after each voltage level was reached, and then removed while the voltage was increased to the next level. This procedure was continued until breakdown occurred. In another series of tests, the magnetic field was present while the voltage was being increased, and then removed at each voltage level.

If the presence of the magnetic field caused a change in breakdown voltage of at least 300 volts (about 1.5%), the breakdowns

would occur more frequently during a particular phase of the testing procedure.

4. Results and Conclusions. A random pattern of behavior was observed. The breakdowns did not consistently occur during a particular phase of either testing cycle. Therefore, it must be concluded that the breakdown voltage does not depend on any effects produced by the primary electrons striking the anode.

Another phenomenon which was observed during the test is worth mentioning. When the direct voltage was sufficiently high and was increased slowly, bright spots appeared at the cathode. These spots disappeared and reappeared at different places on the cathode, but no arcs occurred across the gap.

The explanation of this phenomenon could be that sharp points on the rough surface of the cathode were first heated to the melting temperature of the metal by the field emission current. Then, due to the surface tension in the metal, the sharp points were rounded off and the electric field at the liquified points decreased. This resulted in a decrease in the field-emission intensity and a corresponding decrease in the temperature of the metal point. There was not enough metal evaporated during this process to raise the pressure so that a gaseous breakdown could occur.

C. X-Ray Induced Conductivity.

1. Experimental Procedures. In the previous program it was not possible to make meaningful measurements of x-ray induced conductivity in high-vacuum because all of the available pumping equipment was required for other types of experiments. A few measurements were made on specimens that were being used for a-c loss studies, but, for reasons that are discussed below, the results were only qualitative.

To measure d-c conductivity during irradiation it is necessary that the following conditions be given careful consideration:

- (a) At pressures higher than several microns, ionization current can be high enough to interfere with the measurement of conduction current. In high-vacuum the ionization current is small enough to be neglected.
- (b) Photoelectric emission from exposed metal electrodes can cause currents in the measurement circuit that are as large as the conduction current. It is always necessary to either correct the current readings to account for the net photoelectric current, or to arrange the specimen and its electrodes so that the net photoelectric current in the measurement circuit is small enough to be neglected.
- (c) X-ray absorption in the electrodes can drastically reduce the beam intensity at the specimen surface, particularly when low energy radiation is used. For the 50-KVP x-rays used in this study, it was necessary to apply thin-film electrodes of silver paint or evaporated silver.
- (d) To maintain uniform irradiation throughout the active volume of the specimen it is necessary to limit the specimen thickness. The maximum thickness used in this investigation was 4 mils, so attenuation of the incident beam by absorption in the specimen was small enough to be neglected.
- (e) A long period of electrification is required to permit polarization currents to decay before radiation is

introduced. Furthermore, the specimen must remain electrified at a constant voltage during the entire experiment.

- (f) The temperature of the specimen must be controlled because conductivity depends on temperature. This is particularly important at elevated temperatures.

A cross-sectional view of the specimen/electrode system used in this study is shown in Figure 2. The specimen consists of two layers of dielectric film. Each layer is $3 \frac{1}{8}$ inches in diameter and has a silvered area $2 \frac{3}{4}$ inches in diameter on either side. The silvered areas that are in contact when the films are superimposed serve as measurement electrodes. The silvered areas on the outer faces of the films serve as high-voltage electrodes. Two metal rings that are used to clamp the dielectric films serve as a guard electrode. Electrical connections to the measurement circuit are made as shown in Figure 2.

Photo-electrons emitted from the measurement electrodes are trapped or collected before they can escape from the space between the films, so they make no net contribution to the current in the measurement circuit. Currents caused by emission from other exposed parts do not influence the measured current because they cannot enter the guarded measurement-circuit. Ideally, the radiation should not cause any current in the measurement circuit when the high-voltage electrodes are connected to ground. In practice, this residual current was less than 1% of that measured when the normal voltage was applied.

The specimen/electrode assembly was mounted in a specimen holder and placed in a vacuum chamber so that the front surface of the specimen was perpendicular to the axis of the x-ray beam.

Heating wires located in the back-plate of the holder and in front of the specimen were used to heat the specimen. Thermocouples were used for temperature measurement, and a thermistor was used in the temperature control circuit. The temperature of the specimen was controlled to within 0.1°C at all times.

2. Experimental Results. A complete study of x-ray induced conductivity would include the determination of:

- (a) the instantaneous effects of a sudden increase in radiation intensity.
- (b) the long-time effects of continued irradiation, as measured during irradiation.
- (c) the instantaneous effects of a sudden decrease in radiation intensity.
- (d) the long-time recovery effects.

Each of these characteristics can be affected by the following experimental parameters:

- (a) test voltage
- (b) temperature
- (c) dose rate
- (d) absorbed dose

With the time and facilities that were available for this study, it was not possible to conduct such a complete investigation of induced conductivity, even for one material.

One of the factors studied in the preliminary experiments was the effect of applied voltage on induced conductivity. To measure dark

conductivities of the order of 10^{-20} mho cm^{-1} , it was desirable to make the applied voltage as high as the experimental conditions would permit. Other workers have reported differing voltage effects, depending on the conditions of their respective experiments. Measurements have been reported to show that induced conductivity is ohmic⁽¹²⁾, a decreasing function of voltage⁽¹³⁾, and semi-conductive in nature⁽¹⁴⁾. To determine the relationship between induced conductivity, σ_x , and the applied voltage, V , for the experimental conditions prevailing in this study, measurements were made on three materials over the voltage range from 45 to 320 volts at a dose rate of 550 rads/min (H_2O). At this low dose rate, σ_x reaches a steady value, σ_e , which appears to be an equilibrium value.

These experiments showed that σ_e was non-ohmic. The results for TFE-7, Mylar-C and polyethylene are summarized in Figure 3. These curves indicate a linear relationship between $\log \sigma_e$ and V . This agrees with the results obtained by Amborski⁽¹⁵⁾ on Mylar film at elevated temperatures without irradiation.

Another series of measurements was made to determine the effect of dose rate, R . A typical set of curves for Mylar-C at 68°C is shown in Figure 4. Although the specimens were irradiated for only 10 minutes, each specimen was electrified and heated in the vacuum chamber for 16 hours before irradiation. In all of the results discussed herein, a new sample was used for each set of measurements. This was necessary because thermal and radiation exposure produce permanent effects that influence conductivity.

At the lower dose rates, σ_x appears to reach an equilibrium value, σ_e , as mentioned above. However, at the higher dose rates σ_x goes through a maximum, σ_m . If the irradiation at the lower dose rates is continued long enough, σ_x decreases below the equilibrium value, σ_e . Therefore, the term σ_m is used hereafter to mean the

maximum value of induced conductivity, although this value may persist for a long time when the dose rate is low. These results (Figure 4) indicate the dependence of σ_x on absorbed dose, as well as dose rate.

The relationship between σ_m and dose rate, R , is shown in Figure 5 for TFE-7, Mylar-C and polyethylene. In each case, σ_m follows the relationship discussed in detail by Fowler⁽¹⁶⁾:

$$\sigma_m = bR^\Delta,$$

where σ_m is the maximum value of σ_x , b is a constant and Δ is the slope of the "log σ_m vs. log R " curve, as shown in Figure 5. Fowler related the equilibrium value of σ_x to dose rate for smaller dose rates than those used in this study. However, the relationship holds for the maximum value of σ_x at these higher dose rates. These measurements were, of course, made at a fixed voltage.

Further experiments were conducted to determine the effect of temperature on induced conductivity in Mylar-C. Again, before each radiation exposure, the specimen was electrified and heated to the prescribed temperature in vacuum for 16 hours. The results obtained at temperatures in the range of 68.2 to 92.1°C are summarized in Figure 6. A dose rate of 3600 rads/min was used in all of these experiments.

The dark conductivity is, of course, temperature dependent, and it goes through a maximum during the period following an increase in temperature. In all cases, σ_0 had stabilized before the beginning of the radiation exposure.

At each temperature, σ_x reached a maximum value during the first minute of irradiation. The differences in these maximum values at the various temperatures were of the same order of magnitude as the experimental error. Therefore, measurements at a lower

dose rate would be required to more accurately determine the relationship between σ_m and temperature. However, as the exposure continued, temperature had a drastic effect on the observed behavior.

At the two lower temperatures (68.2 and 75.6°C), σ_x rapidly decayed to a value which then decreased by only 15% during the remainder of the exposure period. At the two higher temperatures, the initial maximum was followed by a broader maximum which occurred during the second hour of irradiation. This second maximum was followed by a steady decrease during the remainder of the exposure period. At an intermediate temperature of 79.7°C, a second maximum was observed, but it took longer to develop and was much broader than those observed at the higher temperatures. A second specimen showed the same behavior at a temperature of 79.8°C.

During these experiments, the pressure in the vacuum chamber was recorded. The chamber was under continuous pumping, so the pressure changes cannot be converted to volumes of released gas. However, the curves of "pressure vs. exposure time", which are shown in Figure 7, indicated that the changes in the measured values of conductivity could be related to the increased pressure in the cell. This unlikely relationship, which would indicate a serious flaw in experimental technique, was tested by placing an additional 100 square inches of Mylar in the chamber and repeating a radiation exposure experiment on a new specimen. The walls of the chamber were heated to 75°C and the conductivity specimen was maintained at 75.6°C. The usual 16 hour pre-irradiation conditioning was carried out. The pressure curve is shown in Figure 7 (broken line). Although this pressure curve is completely out of line with the family of curves for the normal experiments, the conductivity curve (Figure 6) is in line with the other conductivity curves. Therefore, the pressure rise could not have influenced the measured values of induced conductivity.

A considerable amount of work has been reported in the literature on the evolution of gases from various polymers during irradiation, but no information is available on the quantitative identification of gases produced by the irradiation of polyethylene terephthalate.

3. Discussion of Results. Because this investigation is incomplete, several interesting questions must remain unanswered at the moment. As usual, differences in experimental conditions influence the correlation of results with those of other workers. However, in some areas, excellent agreement has been obtained, while in other areas, contradictions seem to be indicated.

The agreement of the " $\log \sigma_x$ vs. V " curves (Figure 3) with the results of Amborski⁽⁴⁾ would indicate that the induced conductivity σ_x , and the dark conductivity, σ_o , are associated with the same conduction mechanism. This relationship, which is interpreted by Amborski and Burton⁽¹⁷⁾ to indicate an ionic transport mechanism, leads to a hyperbolic sine relationship between the conduction current, I , and the applied voltage, V . Their expression is:

$$I = s' \sinh (a'V)$$

where s' and a' are constants.

Fowler⁽¹⁶⁾, on the other hand, found x-ray induced currents to be ohmic, and his analysis of the conduction mechanism is based on conduction by free electrons in the presence of electron traps. In the relationship $\sigma_m = bR^\Delta$, Δ assumes values ranging from 0.5 to 1.0 and is a characteristic of the material. In this model, Δ is related to the distribution of normally forbidden levels, or traps. For a uniform distribution, $\Delta=1$; for an exponential distribution, Δ approaches 0.5. As shown in Figure 5, the values of Δ obtained in this study for TFE-7, Mylar-C and polyethylene were 0.73, 0.83 and

0.66 respectively. These values are in agreement with those of other workers^(12,13,16,18).

Considerably more data would be required to confirm the relationship between σ_m and V over a range of dose rates and temperatures. However, if the linear relationship between $\log \sigma_m$ and V is established, then the constant Δ would also be voltage dependent.

The increase in σ_x to a maximum value, σ_m , during the initial stage of irradiation has been investigated by other workers. Harrison⁽¹⁸⁾ reports that the time, T_0 , required for σ_x to reach a maximum value is related to the dose rate, R , by the expression:

$$T_0 = BR^{-\mu},$$

where B and μ are empirical constants. The time constant, T_0 , is described as the time required for the rate of generation of free carriers to exceed their recombination rate. The data on Mylar-C, shown in Figure 4, does not follow this simple relationship, which implies a linear relationship between $\log T_0$ and $\log R$. The time constant for the lowest dose rate (103 rads/min) is much longer than this relationship would predict. Again, only three points are available and no conclusions can be drawn on such a small amount of data.

The rate at which σ_x decreases after the initial rise has also been investigated by other workers. Coleman⁽¹⁹⁾, using a strontium-90 beta source, found that σ_x decreased according to the relationship:

$$\sigma_x \sim t^{-n},$$

where t is the irradiation time and n depends on the dose rate. This relationship held for polystyrene, monochlorotrifluoroethylene and Corning Vycor 7920 when irradiated at dose rates from 0.05 to 3.0 r/sec. In the present work, a simple exponential function would not

describe the decrease in σ_x with radiation time. As shown in Figure 6, the behavior is more complex, and it depends on temperature as well as dose rate.

Warner, Muller and Nordlin⁽²⁰⁾, using gamma radiation from a Cobalt-60 source at a dose rate of 100r/hr, found a maximum conductivity at about 600 r and decreases thereafter for polyethylene, polystyrene and polytetrafluoroethylene. They suggested that the slow increase in σ_x is associated with a corresponding accumulation of predominately univalent ions, and the subsequent decrease resulted from degradation accompanied by formation of molecular dipoles acting as traps for the ions.

In Figure 6, which shows the effect of temperature on the induced conductivity for a fixed dose rate, it is interesting to note that the difference in behavior (appearance of a second maximum) occurs at temperatures in the range of the second order transition point for polyethylene terephthalate. It would not be expected, however, that any rapid changes in degree of crystallinity would be occurring after 16 hours of conditioning at the prescribed temperatures, unless such changes were induced by the radiation. It is apparent that in this temperature region, even small changes in temperatures produce significant effects on the variation of σ_x with irradiation time. A detailed study of the effects of temperature and degree of crystallinity on induced conductivity might reveal further information on the conduction and degradation mechanisms.

As mentioned previously, time would not permit a thorough study of x-ray induced conductivity in polymers. Several questions arise concerning the correlation of the available data on polyethylene terephthalate with the published work of other investigators. The results of this incomplete study immediately suggest several further experiments that would lead to useful conclusions.

D. X-Ray Induced A-C Losses.

1. Previous Results. In the previous program, measurements of dielectric constant and dissipation factor ($\tan\delta$) were made on several materials during x-ray irradiation in high-vacuum. The largest effects were those exhibited by the polytetrafluoroethylene materials TFE-6 and TFE-7. Large increases in dielectric constant and $\tan\delta$ were observed at frequencies up to 1 kc during irradiation. The results obtained on TFE-6 in vacuum and in air are summarized in Figures 8 and 9.

Curve B is typical of the behavior of both TFE-6 and TFE-7, where a maximum value of $\tan\delta$ was reached during the early stages of exposure, followed by a decrease during the remainder of the exposure period in vacuum. When irradiated in air (Curve A), the high value of $\tan\delta$ was maintained throughout the exposure period. A specimen that had previously been exposed (8.5 megarads) and allowed to recover for 10 months (Curve C) showed the same general behavior during the second irradiation, but the increase in $\tan\delta$ was moderated and a steady value was observed during the latter part of the second exposure period.

The recovery data of Figure 9 shows a marked difference between the vacuum-irradiated and air-irradiated specimens. $\tan\delta$ decreased during the 30-day recovery period for the specimen irradiated in air (Curve A). The rate of decay decreased during the recovery period ($\tan\delta$ plotted on logarithm scale), but there was a continuous decay. The specimens irradiated in vacuum (Curves B and C) showed a sudden decrease in $\tan\delta$ when the irradiation was removed, followed by a constant value of $\tan\delta$ during a 5-day recovery period in vacuum. However, when the pressure in the chamber was returned to one atmosphere, both specimens showed a sudden increase in $\tan\delta$. After a period of somewhat erratic behavior for the specimen of Curve B,

$\tan\delta$ remained constant for both specimens during the remainder of the 30-day exposure period; Curve C being a decade higher than Curve B.

Attempts to explain these results on the basis of the known radiation effects on the structure of the polymer were not successful. One complication was associated with the data obtained on an old lot of polytetrafluoroethylene that had been stored in the laboratory for several years. This material did not exhibit the drastic effects observed with TFE-6 and TFE-7, yet its structure was essentially the same. In an effort to more accurately define the factors that contribute to the drastic effects exhibited by TFE-6 and TFE-7, further experiments were conducted during the present program.

2. Experimental Results. To determine if diffusion of gases contributes to the observed behavior, specimens of different thicknesses were irradiated. A 30-mil specimen and a 125-mil specimen were machined from the same 1/2 inch thick block of TFE-7. A second 30-mil specimen was taken from a sheet of 30-mil skived film, which was also made of TFE-7. Dielectric constant and $\tan\delta$ measurements were made over the frequency range of 100 cps to 100 kc. The 100 cps $\tan\delta$ data is summarized in Figure 10.

The inclusion of the 30-mil film proved to be fortuitous because it behaved in a manner that was totally unexpected and indicated that the processing of the resins plays an important role in radiation effects. The two machined samples followed the same general pattern that had been previously observed with TFE-6 and TFE-7 specimens. The skived film, on the other hand, showed an entirely different behavior, as shown in Figure 10. Its $\tan\delta$ did not rapidly increase to the high values exhibited by the machined specimens. Rather, it exhibited a slow increase in $\tan\delta$ during the entire exposure

period (480 hours, 12.3 megarads). During the latter part of the exposure period, the increasing $\tan\delta$ of the film was considerably higher than the decreasing $\tan\delta$ of the machined specimens.

The recovery data, shown in Figure 11, also indicates a marked difference in behavior between the two types of specimens. The film, which had never reached a peak value of $\tan\delta$ during irradiation, exhibited a steady decrease in $\tan\delta$ during the 20-day recovery period in high-vacuum. The machined specimens showed a more rapid decrease in $\tan\delta$ followed by a period of little change. The 30-mil machined specimen did exhibit a more rapid decay in $\tan\delta$ than the 125-mil specimen, and this may well be the most significant effect of the reduced thickness.

When the cell was filled with dry (oil pumped) nitrogen, a sudden increase in $\tan\delta$ was observed for all three specimens. This effect had been observed in all previous experiments with the TFE polymers. The effect was somewhat moderated in the case of the skived film, but the pattern of behavior was essentially the same.

It should be noted that the skived film did exhibit a small peak in the $\tan\delta$ curve during the early part of the radiation exposure period. This peak may be significant, and it is referred to later in the discussion.

Corresponding changes in dielectric constant were observed and they are shown in Figures 12 and 13.

The effects are greatly moderated at 1 kc, where the maximum value of $\tan\delta$ during exposure was 0.0018 for the 30-mil machined specimen, and 0.020 for the 125-mil machined specimen. All of the detailed data are given in Tables 1 to 4.

It was suggested by the manufacturer that the primary difference between the machined specimens and the skived films is associated with the sintering process. The film is skived from a large diameter cylinder after the sintering process is completed. Therefore, a specimen taken from the outer portion of the cylinder would have been exposed to air during sintering, while a specimen taken from the inner portion of the solid cylinder would have been protected from the atmosphere. There was no way of determining the location from which the specimen used in this experiment had been taken, but another experiment provided data that confirms the suggestion that the presence of oxygen during sintering influences the observed radiation effects.

Two types of TFE-7 specimens supplied by E. I. du Pont de Nemours and Company were used in this phase of the investigation. They are identified as follows:

A-2 Sintered in air, 380°C , 2 hours.

N-2 Sintered in nitrogen, 380°C 2 hours.

A-16 Sintered in air, 380°C , 16 hours.

N-16 Sintered in nitrogen, 380°C , 16 hours.

The results obtained at 100 cps are shown in Figures 14 to 17. In Figure 14, the specimen sintered for 2 hours in nitrogen exhibited a behavior similar to that of the 30-mil skived film, while the specimen sintered for 2 hours in air showed effects similar to those that had been observed for all other TFE specimens. Again, the small peak in the $\tan\delta$ curve was observed during the early stages of exposure.

The $\tan\delta$ recovery data (Figure 15) showed the same pattern of behavior that had been previously observed. The recovery period in high-vacuum was extended to 55 days, but no large changes occurred during the latter part of this period. Again, $\tan\delta$ increased when the cell was filled with dry nitrogen.

The detailed data, given in Tables 5 to 8, shows that the effects were greatly moderated at 1 kc. This same frequency effect has been observed in all of the experiments with the TFE polymers.

The only other material that is reported to show effects similar to the TFE resins is a composition of methyl styrene with a small amount of dimethyl siloxane additive. These results were reported by Pendergast and Hoffman⁽²¹⁾. Specimens of similar composition, identified as C-1147, were obtained from the Delaware Research and Development Corporation, Wilmington, Delaware. During x-ray irradiation for 338 hours in high-vacuum (6 megarads), the dielectric constant of C-1147 remained at a value of 2.55 and the highest value of $\tan\delta$ measured at 100 cps was 0.0005. No changes occurred when the radiation was removed.

After venting the cell to the atmosphere, the same specimens were exposed in air for an additional 382 hours (3.6 megarads). The only effect produced was an immediate rise in the measured value of $\tan\delta$ to 0.003 at 100 cps. This increase was caused by the ionization current parallel to the specimen. $\tan\delta$ immediately returned to its normal value when the x-ray generator was turned off.

Since the effects reported by Pendergast and Hoffman were not evident under the experimental conditions of this investigation, no correlation could be made with the behavior of the TFE resins.

3. Discussion of Results. The additional data obtained in the present program shows that an explanation of the effects of radiation on the a-c loss properties of the TFE resins must include the role of end-groups and, perhaps, impurities. The simple considerations of breaking C-C bonds and C-F bonds to form ions or free radicals do not account for the observed behavior. The high induced losses may be associated with conduction in the presence of traps, but the nature of the charge transport mechanism has not been identified.

It has been shown that the results of an irradiation experiment on the TFE resins are drastically affected by the processing methods used in fabricating the specimens. This is certainly illustrated by the data of Figure 10, which shows that after an absorbed dose of 2.5 megarads the 30-mil skived film had a $\tan\delta$ of 0.0005, while the 30-mil machined specimen had a $\tan\delta$ that was two decades higher (0.05). Furthermore, during the period when $\tan\delta$ was steadily increasing with one type of material, it was decreasing with the other type. Therefore, even the qualitative results of an irradiation study are influenced by the manufacturing process.

Additional information would be required to explain the high induced losses in the TFE resins. The x-ray induced conductivity of these materials is comparable to that observed with other polymers, yet these other materials do not exhibit induced a-c losses. Therefore, it is not a simple conduction mechanism that causes the high induced losses.

From the practical viewpoint, it should be noted that the large changes in $\tan\delta$ caused by irradiation occur only at low frequencies. The effect is greatly moderated at 1 kc, and measurements on a group of specimens that had high dissipation factors after irradiation showed no significant increase in losses in the frequency range from 1.0 to 10 Mc. It is also important to note that the copolymer of tetrafluoroethylene and hexafluoropropylene, FEP, did not exhibit any changes in a-c properties as a result of x-ray irradiation.

E. Electric Strength Measurements. A considerable amount of data on the electric strength of solid materials at frequencies up to 100 Mc has been collected during the course of several investigations at this laboratory. A practical interpretation of these data has been summarized in a single Government report⁽²²⁾ and a published paper⁽²³⁾. In these previous measurements, various types of specimens

with recessed electrodes were used to eliminate the compromising effects of corona in the surrounding medium. In the present program, a specimen has been developed which will permit more complete evaluation of the factors that may influence the frequency dependence of electric strength. A cross-sectional view of the specimen is shown in Figure 18.

The important feature of this specimen is the shape of the cavity. The thinnest section is located at the base of the circular groove. Therefore, the raised section at the center of the cavity, where machining is most difficult, is not involved in the breakdown. The tubular high-voltage electrode makes contact with a silver coating in the cavity, but does not rest on the bottom of the circular groove. To be sure that good contact is made, continuity between the raised section of the cavity and the tubular electrode is checked with an ohmmeter. A silvered area on the bottom of the specimen is placed in contact with a ground electrode.

The specimen is fabricated from a $1/2'' \times 1\ 3/4'' \times 1\ 3/4''$ block. The cavity is started with a $3/4''$ diameter drill and then finished with a special tool in a lathe. The tool has a semi-circular tip ($1/8''$ radius) which forms the groove at the base of the cavity. The specimen is mounted on a precision-ground backing plate that is held in the lathe chuck. A countersunk hole in each corner of the specimen permits machine screws to be used in mounting the specimen on the backing plate. This plate, which extends beyond the edges of the specimen, is used as a reference point in determining the depth of penetration of the tool to obtain a given thickness at the base of the cavity.

Preliminary tests on polystyrene specimens have been successful. Values of electric strength as high as 2600 VPM at 2 Mc have been obtained with a breakdown thickness of 5 mils. The breakdowns consistently occur at the base of the groove, in the thinnest section of the

specimen. Polystyrene was chosen for the preliminary tests because it has the highest known electric strength in the r-f range, it is more difficult to machine than most polymers, and its transparency permits optical examination of the material in the critical part of the specimen.

This specimen offers a great deal of versatility in the selection of breakdown thickness, thickness of metallic coating, and thermal conductivity of electrodes. It should prove to be useful in future breakdown studies.

IV. Conclusions.

When the present program was initiated, it was not anticipated that circumstances would make it necessary to discontinue the investigation at the close of the current reporting period. Consequently, certain phases of the program are incomplete, and only a few final conclusions can be drawn. However, the results obtained during this period are summarized as follows:

1. Vacuum sparkover measurements in the presence of a strong magnetic field have shown that the breakdown voltage does not depend on effects produced by primary electrons striking the anode.
2. X-ray induced conductivity, σ_x , in Mylar-C, TFE-7 and polyethylene was voltage dependent when measured at a dose rate of 550 rads/min (H_2O). The maximum (or equilibrium) value followed the relationship $\log \sigma_m \sim V$.
3. For dose rates between 100 and 5000 rads/min (H_2O) σ_m was related to dose rate, R , by the expression $\sigma_m = bR^\Delta$. The values of Δ for TFE-7, Mylar-C and polyethylene were 0.73, 0.83 and 0.66 respectively, when measured at a fixed voltage.
4. The time, T_o , required for σ_x (Mylar-C) to reach a maximum value, σ_m , did not follow the simple relationship $T_o = BR^{-\mu}$, where R is the dose rate, and B and μ are empirical constants.

5. The decay in σ_x after the initial rise to σ_m , did not follow a simple exponential for Mylar-C.
6. Temperature has a significant effect on σ_x for Mylar-C. A second maximum in the " σ_x vs. absorbed dose" curve is observed when the experiment is conducted at temperatures above the second order transition point.
7. Irradiation effects on the loss properties of TFE polymers are greatly influenced by the presence of oxygen during the sintering process. Explanation of the observed behavior must be concerned with end-groups and, perhaps, impurities.
8. Diffusion (specimen thickness) has little effect on the x-ray induced losses in TFE-7.
9. X-ray irradiation did not affect the loss properties of a composition of methyl styrene with a small amount of dimethyl siloxane additive, for absorbed doses up to 9.6 megarads.

V. Recommendations.

This investigation will not be continued under USAERDL sponsorship, so specific recommendations concerning an extension of the work would not be appropriate. Some phases of the study will be continued under the sponsorship of the National Aeronautics and Space Administration, George C. Marshall Space Flight Center, Huntsville, Alabama.

VI. Cited References.

1. F. Llewellyn-Jones, Ionization and Breakdown in Gases. John Wiley and Sons, Inc., New York, New York.
2. L.J. Frisco, Dielectrics for Satellites and Space Vehicles, Final Report Contract DA-36-039-SC-78321, March 1, 1959 - February 28, 1962, Dielectrics Laboratory, The Johns Hopkins University, Baltimore, Maryland.
3. W.P. Dyke, J.K. Trolan, Field Emission: Large Current Densities, Space Charge, and the Vacuum Arc. Phys. Rev., Vol. 89, No. 4 (1953).
4. W.P. Dyke, J.K. Trolan, E.E. Martin and J.P. Barbour, The Field Emission Initiated Vacuum Arc I. Experiments on Arc Initiation. Phys. Rev., Vol. 91, No. 5 (1953).
5. W.W. Dolan, W.P. Dyke and J.K. Trolan, The Field Emission Initiated Vacuum Arc II. The Resistively Heated Emitter. Phys. Rev., Vol. 91, No. 5 (1953).
6. J.W. Beams, Field Electron Emission From Liquid Mercury. Phys. Rev., 44, 803 (1933).
7. W.S. Boyle, P. Kisliuk and Z.H. Germer, Electrical Breakdown in High Vacuum. J. Appl. Phys., Vol. 26, 720 (1955).
8. L.V. Tarasova, Present-Day Ideas Concerning the Mechanism of Electrical Breakdown in High Vacuum. NASA TTF-42, Washington, D.C., October 1960. Technical Translation F-42 from Uspekhi fizicheskikh Nauk, Vol. 58, No. 2 (1956).
9. A.I. Bennet, Electron Multiplication Processes in High Voltage Electrical Discharge in Vacuum. J. Appl. Phys., Vol. 28, No. 11 (1957).
10. Lawrence Cranberg, The Initiation of Electrical Breakdown in Vacuum. J. Appl. Phys., Vol. 23, 518 (1952).
11. Paul Kisliuk, Arc at Electrical Contacts on Closure. The Cathode Mechanism of Extremely Short Arcs. J. Appl. Phys., Vol. 25, No. 7 (1954).
12. F.A. Muller and H.G. Nordlin, The Effects of Ionizing Radiation on the Electrical Conductivity of High Quality Insulation Materials, 1952 Annual Report of the Conference on Electrical Insulation, NAS-NRC, p. 32 (1953).

13. W.E. Loy, Jr., Effects of Gamma Radiation on Some Electrical Properties of TFE-Fluorocarbon Plastics. Materials in Nuclear Applications, ASTM Special Publication No. 276, p.68-78 (1960).
14. J.C. Pigg, C.D. Bopp, O. Sisman and C.C. Robinson, The Effects of Reactor Irradiation on Electrical Insulation. Communications and Electronics, No. 22, p.717-23 (1956).
15. L.E. Amborski, Structural Dependence of the Electrical Conductivity of Polyethylene Terephthalate. J. Polymer Sci., Vol. 62, 331-46 (1962).
16. J.F. Fowler, X-Ray Induced Conductivity in Insulating Materials. Proceedings of the Roayl Society, Vol. 236A, p.464-80 (1956).
17. L.E. Amborski and R.L. Burton, High Temperature Resistivity of Polyethylene Terephthalate Film. 1953 Annual Report of the Conference on Electrical Insulation, NAS-NRC, p.28 (1954).
18. S.E. Harrison, Measured Behavior of Gamma-Ray Photoconductivity in Organic Dielectrics. AIEE Conference Paper CP-62-1251 (1962).
19. J.H. Coleman, Effects of Beta Radiation on the D-C Conductivity of Good Insulators. 1954 Annual Report of the Conference on Electrical Insulation, NAS-NRC, p.51 (1955).
20. A.J. Warner, F.A. Muller and H.G. Nordlin, Electrical Conductivity Induced by Ionizing Radiation in Some Polymeric Materials. Letter to the Editor, J. of Appl. Phys., Vol. 25, p.131 (1954).
21. H.E. Pendergast and A.S. Hoffman, Tensile, Impact and Dielectric Properties of Irradiated Polymers. AIEE Conference Paper 61-391, presented at AIEE Winter General Meeting, January 29 - February 3, 1961.
22. J.J. Chapman and L.J. Frisco, A Practical Interpretation of Dielectric Measurements Up To 100-Mc. Final Report of Contract DA-36-039-SC-73156, December 31, 1958.
23. L.J. Frisco, Frequency Dependence of Electric Strength - A Design Consideration Analysis. Electro-Technology, Vol. 68, No. 8, p. 110-17 (1961).

VII. Identification of Personnel.

L. J. Frisco	Research Contract Director, M. Sc. in Electrical Engineering. Full time.
A. M. Muhlbaum	Research Associate, Dipl. in Engineering Physics (Technical University of Delft, Netherlands). Full time.
E. A. Szymkowiak	Research Staff Assistant, B. E. in Electrical Engineering. Full time.
W. G. Baumann	Research Technician. Full time.
Duncan McCulloch	Research Technician. Full time.
C. L. Woodward	Secretary. Full time.

VIII. Acknowledgements.

The investigation of radiation effects on polytetrafluoroethylene was conducted in close cooperation with the Polychemicals Department, E.I. du Pont de Nemours and Company, Wilmington, Delaware. Their assistance and keen interest in the program is appreciated.

The following organizations contributed specimens and offered technical assistance whenever it was requested:

E.I. du Pont de Nemours and Company
Polyester Film Research and Development
Department
Circleville, Ohio

Delaware Research and Development Corporation
Wilmington, Delaware

IX. Tables.

<u>Table</u>	<u>Description</u>	<u>Page</u>
1	TFE-7 Vacuum X-Ray Exposure and Recovery Data, 100 cps.	43
2	TFE-7 Vacuum X-Ray Exposure and Recovery Data, 1 kc.	44
3	TFE-7 Vacuum X-Ray Exposure and Recovery Data, 10 kc.	45
4	TFE-7 Vacuum X-Ray Exposure and Recovery Data, 100 kc.	46
5	TFE-7 Vacuum X-Ray Exposure and Recovery Data, 100 cps. Effect of sintering.	47
6	TFE-7 Vacuum X-Ray Exposure and Recovery Data, 1 kc. Effect of sintering.	48
7	TFE-7 Vacuum X-Ray Exposure and Recovery Data, 10 kc. Effect of sintering.	49
8	TFE-7 Vacuum X-Ray Exposure and Recovery Data, 100 kc. Effect of sintering.	50

TABLES

43

Table 1. TFE-7 Vacuum X-Ray Exposure and Recovery Data, 100 cps.

A - 30-mil skived film.
B - 30-mil machined.
C - 125-mil machined.

Exposure Time (Hours)	Dissipation Factor			Dielectric Constant			Absorbed Dose (Mrads)
	A	B	C	A	B	C	
0	.0003	.0003	.0003	2.083	2.101	2.10	0
6	.0003	.043	.108	2.083	2.153	2.16	.15
22	.0003	.061	.135	2.083	2.179	2.25	.54
28	.0004	.067	.140	2.085	2.197	2.24	.70
30	.0004	.071	.145	2.087	2.207	2.24	.75
47	.0004	.072	.122	2.087	2.181	2.22	1.18
54	.0004	.071	.105	2.087	2.167	2.21	1.36
71	.0004	.063	.077	2.087	2.157	2.19	1.78
78	.0004	.057	.062	2.087	2.155	2.18	1.96
94	.0005	.044	.043	2.087	2.143	2.16	2.36
102	.0005	.039	.036	2.087	2.141	2.16	2.51
166	.0008	.014	.011	2.087	2.119	2.16	4.16
173	.0008	.013	.0078	2.087	2.117	2.16	4.34
190	.0010	.010	.0080	2.087	2.117	2.16	4.77
197	.0011	.0095	.0074	2.087	2.115	2.16	4.94
214	.0012	.0080	.0063	2.087	2.111	2.16	5.37
221	.0013	.0075	.0058	2.087	2.111	2.16	5.55
235	.0014	.0065	.0051	2.087	2.111	2.16	5.90
257	.0018	.0052	.0042	2.089	2.111	2.16	6.45
324	.0048	.0028	.0025	2.089	2.111	2.16	8.14
329	.0053	.0026	.0023	2.089	2.111	2.16	8.26
346	.0062	.0020	.0016	2.089	2.111	2.16	8.68
354	.0068	.0018	.0014	2.089	2.111	2.16	8.88
419	.0085	.0012	.0010	2.093	2.111	2.16	10.5
425	.0087	.0012	.0010	2.095	2.111	2.16	10.7
490	.012	.0011	.0010	2.097	2.111	2.16	12.3
Recovery							
Time (Hours)							
0	.0120	.0011	.0010	2.097	2.111	2.16	
2	.0115	.0010	.0009	2.097	2.111	2.16	
6	.0105	.0007	.0009	2.097	2.111	2.16	
24	.0081	.0004	.0008	2.093	2.111	2.16	
48	.0055	.0003	.0006	2.091	2.111	2.16	
72	.0045	.0003	.0005	2.091	2.111	2.16	
96	.0035	.0003	.0005	2.089	2.111	2.16	
168	.0023	.0003	.0004	2.087	2.111	2.16	
192	.0021	.0003	.0004	2.087	2.111	2.16	
216	.0019	.0003	.0004	2.087	2.111	2.16	
240	.0016	.0003	.0004	2.087	2.111	2.16	
264	.0015	.0003	.0004	2.087	2.111	2.16	
336	.0009	.0002	.0003	2.087	2.111	2.16	
360	.0008	.0002	.0003	2.087	2.111	2.16	
384	.0006	.0002	.0003	2.087	2.111	2.16	
504	.0002	.0002	.0003	2.087	2.111	2.16	
*510	.019	.070	.026	2.097	2.279	2.20	
528	.016	.096	.062	2.097	2.263	2.24	
552	.014	.080	.084	2.097	2.203	2.27	
600	.010	.057	.065	2.097	2.183	2.22	
744	.0085	.039	.045	2.095	2.175	2.21	
1032	.0076	.034	.042	2.093	2.143	2.19	
1104	.0073	.033	.042	2.093	2.141	2.19	
1248	.0069	.031	.040	2.093	2.141	2.19	
1416	.0065	.029	.039	2.091	2.141	2.19	
1920	.0050	.023	.036	2.091	2.139	2.19	

* - Recovery through 504 hours in vacuum; subsequent data obtained in dry nitrogen at atmospheric pressure.

TABLES

Table 2. TFE-7 Vacuum X-Ray Exposure and Recovery Data, 1 kc.

A - 30-mil skived film,
 B - 30-mil machined,
 C - 125-mil machined.

Exposure Time (Hours)	Dissipation Factor			Dielectric Constant			Absorbed Dose (Mrads)
	A	B	C	A	B	C	
0	.0003	.0003	.0003	2.081	2.099	2.10	0
6	.0003	.0061	.015	2.081	2.105	2.15	.15
22	.0003	.0085	.018	2.081	2.107	2.17	.54
28	.0003	.0105	.020	2.083	2.111	2.16	.70
47	.0003	.0088	.016	2.085	2.111	2.15	1.18
54	.0003	.0085	.015	2.085	2.115	2.15	1.36
71	.0003	.0072	.010	2.085	2.111	2.15	1.78
78	.0003	.0065	.009	2.085	2.111	2.15	1.96
94	.0003	.0053	.0058	2.085	2.111	2.15	2.36
102	.0003	.0047	.0044	2.085	2.109	2.15	2.51
166	.0003	.0017	.0017	2.085	2.109	2.15	4.16
173	.0003	.0015	.0016	2.085	2.109	2.15	4.34
190	.0003	.0014	.0015	2.085	2.109	2.16	4.77
197	.0003	.0013	.0015	2.085	2.109	2.16	4.94
214	.0004	.0012	.0014	2.037	2.109	2.16	5.37
221	.0004	.0012	.0014	2.087	2.109	2.16	5.55
235	.0004	.0011	.0014	2.087	2.109	2.16	5.90
257	.0006	.0010	.0012	2.087	2.109	2.16	6.45
324	.0009	.0005	.0009	2.087	2.109	2.16	8.14
329	.0009	.0005	.0008	2.087	2.109	2.16	8.26
346	.0010	.0005	.0008	2.087	2.109	2.16	8.68
354	.0010	.0004	.0008	2.087	2.109	2.16	8.88
419	.0015	.0004	.0008	2.087	2.109	2.16	10.5
425	.0015	.0004	.0008	2.087	2.109	2.16	10.7
490	.0013	.0004	.0008	2.087	2.109	2.16	12.3
Recovery							
Time (Hours)	A	B	C	A	B	C	
0	.0018	.0004	.0008	2.087	2.111	2.16	
2	.0018	.0002	.0008	2.087	2.111	2.16	
6	.0017	.0002	.0008	2.087	2.111	2.16	
24	.0013	.0002	.0008	2.087	2.111	2.16	
48	.0010	.0002	.0008	2.087	2.111	2.16	
72	.0009	.0002	.0008	2.085	2.111	2.16	
96	.0008	.0002	.0008	2.085	2.111	2.16	
168	.0006	.0002	.0008	2.085	2.111	2.16	
192	.0005	.0002	.0008	2.085	2.111	2.16	
216	.0005	.0002	.0008	2.085	2.111	2.16	
240	.0004	.0002	.0008	2.085	2.111	2.16	
264	.0003	.0002	.0008	2.085	2.111	2.16	
336	.0003	.0002	.0008	2.085	2.111	2.16	
360	.0003	.0002	.0008	2.085	2.111	2.16	
384	.0003	.0002	.0008	2.085	2.111	2.16	
504	.0002	.0002	.0008	2.085	2.111	2.16	
*510	.0020	.014	.0056	2.085	2.123	2.16	
528	.0025	.015	.011	2.085	2.123	2.16	
552	.0020	.011	.015	2.087	2.117	2.16	
600	.0016	.0084	.010	2.087	2.117	2.16	
744	.0013	.0060	.0075	2.087	2.115	2.16	
1032	.0012	.0049	.0070	2.087	2.115	2.16	
1104	.0012	.0045	.0069	2.087	2.115	2.16	
1248	.0011	.0042	.0066	2.087	2.115	2.16	
1416	.0011	.0040	.0065	2.087	2.115	2.16	
1920	.0009	.0035	.0058	2.087	2.115	2.16	

* - Recovery through 504 hours in vacuum; subsequent data obtained in dry nitrogen at atmospheric pressure.

Table 3. TFE-7 Vacuum X-Ray Exposure and Recovery Data, 10 kc.

A - 30-mil skived film.
 B - 30-mil machined.
 C - 125-mil machined.

Exposure Time (Hours)	Dissipation Factor			Dielectric Constant			Absorbed Dose (Mrads)
	A	B	C	A	B	C	
0	.0003	.0003	.0003	2.081	2.099	2.10	0
6	.0003	.0008	.0021	2.081	2.101	2.14	.15
22	.0003	.0012	.0029	2.081	2.105	2.15	.54
28	.0002	.0013	.0030	2.083	2.105	2.15	.70
47	.0002	.0014	.0025	2.083	2.105	2.14	1.18
54	.0002	.0014	.0023	2.083	2.105	2.14	1.36
71	.0003	.0012	.0018	2.083	2.105	2.14	1.78
78	.0003	.0011	.0016	2.083	2.105	2.14	1.96
94	.0003	.0008	.0012	2.083	2.105	2.14	2.36
102	.0003	.0007	.0010	2.083	2.105	2.14	2.51
166	.0003	.0003	.0007	2.083	2.105	2.14	4.16
173	.0003	.0003	.0007	2.083	2.105	2.14	4.34
190	.0003	.0003	.0007	2.083	2.107	2.15	4.77
197	.0003	.0003	.0007	2.085	2.107	2.15	4.94
214	.0003	.0002	.0007	2.085	2.107	2.15	5.37
235	.0003	.0002	.0006	2.085	2.107	2.15	5.90
257	.0003	.0002	.0006	2.085	2.107	2.15	6.45
324	.0004	.0002	.0005	2.085	2.107	2.15	8.14
329	.0004	.0002	.0005	2.085	2.107	2.15	8.26
346	.0004	.0002	.0005	2.085	2.107	2.15	8.68
419	.0004	.0002	.0005	2.085	2.107	2.15	10.5
425	.0004	.0002	.0005	2.085	2.107	2.15	10.7
490	.0004	.0002	.0005	2.085	2.107	2.15	12.3
Recovery							
Time (Hours)	A	B	C	A	B	C	
0	.0005	.0002	.0005	2.085	2.109	2.15	
24	.0005	.0002	.0005	2.085	2.109	2.15	
48	.0004	.0002	.0005	2.085	2.109	2.15	
72	.0004	.0002	.0005	2.085	2.109	2.15	
96	.0004	.0002	.0005	2.085	2.109	2.15	
168	.0004	.0002	.0005	2.083	2.109	2.15	
192	.0004	.0002	.0005	2.083	2.109	2.15	
216	.0004	.0002	.0005	2.083	2.109	2.15	
240	.0004	.0002	.0005	2.083	2.109	2.15	
264	.0004	.0002	.0005	2.083	2.109	2.15	
336	.0004	.0002	.0005	2.083	2.109	2.15	
360	.0004	.0002	.0005	2.083	2.109	2.15	
504	.0004	.0002	.0005	2.083	2.109	2.15	
*510	.0005	.0024	.0013	2.085	2.109	2.15	
528	.0007	.0022	.0023	2.085	2.109	2.15	
552	.0006	.0015	.0025	2.085	2.109	2.15	
744	.0005	.0008	.0016	2.085	2.109	2.15	
1248	.0004	.0008	.0014	2.085	2.109	2.15	
1920	.0004	.0007	.0012	2.085	2.109	2.15	

* - Recovery through 504 hours in vacuum; subsequent data obtained in dry nitrogen at atmospheric pressure.

Table 4. TFE-7 Vacuum X-Ray Exposure and Recovery Data, 100 kc.

A - 30-mil skived film.
 B - 30-mil machined.
 C - 125-mil machined.

Exposure Time (Hours)	Dissipation Factor			Dielectric Constant			Absorbed Dose (Mrads)
	A	B	C	A	B	C	
0	.0002	.0002	.0002	2.081	2.097	2.09	0
6	.0002	.0002	.0007	2.081	2.099	2.14	.15
22	.0002	.0002	.0010	2.081	2.105	2.15	.54
28	.0002	.0002	.0011	2.081	2.105	2.15	.70
47	.0002	.0002	.0012	2.083	2.105	2.14	1.18
54	.0002	.0002	.0012	2.083	2.105	2.14	1.36
71	.0002	.0002	.0010	2.083	2.105	2.14	1.78
78	.0002	.0002	.0010	2.083	2.105	2.14	1.96
94	.0002	.0002	.0008	2.083	2.105	2.14	2.36
102	.0002	.0002	.0007	2.083	2.105	2.14	2.51
166	.0002	.0002	.0006	2.083	2.105	2.14	4.16
173	.0002	.0002	.0006	2.083	2.105	2.14	4.34
190	.0002	.0002	.0006	2.083	2.107	2.15	4.77
197	.0002	.0002	.0006	2.085	2.107	2.15	4.94
214	.0002	.0003	.0005	2.085	2.107	2.15	5.37
235	.0002	.0003	.0004	2.085	2.107	2.15	5.90
257	.0002	.0003	.0004	2.085	2.107	2.15	6.45
324	.0002	.0003	.0004	2.085	2.107	2.15	8.14
329	.0002	.0003	.0004	2.085	2.107	2.15	8.26
346	.0002	.0003	.0004	2.085	2.107	2.15	8.68
419	.0002	.0003	.0004	2.085	2.107	2.15	10.5
425	.0002	.0003	.0004	2.085	2.107	2.15	10.7
490	.0002	.0003	.0004	2.085	2.107	2.15	12.3
Recovery							
Time (Hours)							
0	.0003	.0002	.0004	2.085	2.109	2.15	
24	.0003	.0002	.0004	2.085	2.109	2.15	
48	.0003	.0002	.0004	2.085	2.109	2.15	
72	.0003	.0002	.0004	2.085	2.109	2.15	
96	.0003	.0002	.0004	2.085	2.109	2.15	
168	.0003	.0002	.0004	2.083	2.109	2.15	
192	.0003	.0002	.0004	2.083	2.109	2.15	
216	.0003	.0002	.0004	2.083	2.109	2.15	
240	.0003	.0002	.0004	2.083	2.109	2.15	
264	.0003	.0002	.0004	2.083	2.109	2.15	
336	.0003	.0002	.0004	2.083	2.109	2.15	
360	.0003	.0002	.0004	2.083	2.109	2.15	
504	.0003	.0002	.0004	2.083	2.109	2.15	
*510	.0003	.0002	.0004	2.085	2.109	2.15	
528	.0004	.0003	.0005	2.085	2.109	2.15	
552	.0004	.0004	.0009	2.085	2.109	2.15	
744	.0004	.0004	.0007	2.085	2.109	2.15	
1248	.0004	.0004	.0005	2.085	2.109	2.15	
1920	.0004	.0004	.0005	2.085	2.109	2.15	

* - Recovery through 504 hours in vacuum; subsequent data obtained in dry nitrogen at atmospheric pressure.

Table 5. TFE-7 Vacuum X-Ray Exposure and Recovery Data, 100 cps.

Exposure Time (Hours)	Dissipation Factor				Dielectric Constant				Absorbed Dose (Mrads)
	A-2	N-2	A-16	N-16	A-2	N-2	A-16	N-16	
0	.0004	.0005	.0005	.0005	2.165	2.13	2.190	2.210	0
7	.028	.0008	.054	.0023	2.175	2.13	2.200	2.210	.18
23	.065	.0011	.036	.0047	2.205	2.13	2.200	2.210	.58
32	.069	.0008	.029	.0065	2.205	2.13	2.200	2.210	.80
47	.062	.0006	.021	.0097	2.195	2.13	2.200	2.210	1.18
73	.059	.0011	.012	.015	2.195	2.13	2.190	2.210	1.83
85	.051	.0031	.0095	.017	2.195	2.13	2.190	2.210	2.13
168	.030	.021	.0032	.016	2.175	2.13	2.190	2.210	4.22
192	.025	.026	.0024	.016	2.175	2.14	2.190	2.210	4.83
215	.022	.031	.0021	.017	2.175	2.14	2.190	2.220	5.40
242	.018	.031	.0018	.017	2.175	2.14	2.190	2.220	6.08
266	.017	.031	.0017	.017	2.175	2.14	2.190	2.220	6.67
336	.011	.034	.0013	.016	2.175	2.14	2.190	2.220	8.44
360	.0097	.033	.0013	.014	2.175	2.14	2.190	2.220	9.03
384	.0086	.032	.0013	.012	2.175	2.14	2.190	2.220	9.64
408	.0078	.028	.0013	.011	2.175	2.14	2.190	2.220	10.2
503	.0045	.028	.0013	.0072	2.175	2.14	2.190	2.220	12.6
552	.0039	.024	.0013	.0066	2.175	2.14	2.190	2.220	13.8
597	.0038	.020	.0013	.0061	2.175	2.14	2.190	2.220	15.0
668	.0038	.020	.0013	.0055	2.175	2.13	2.190	2.220	16.7
Recovery Time (Hours)									
24	.0034	.018	.0013	.0038	2.175	2.13	2.190	2.220	
72	.0017	.018	.0013	.0031	2.175	2.13	2.190	2.220	
96	.0015	.017	.0013	.0028	2.175	2.13	2.190	2.220	
168	.0015	.016	.0013	.0023	2.175	2.13	2.190	2.220	
264	.0014	.014	.0013	.0022	2.175	2.13	2.190	2.220	
360	.0014	.013	.0012	.0022	2.175	2.13	2.190	2.220	
480	.0013	.013	.0011	.0022	2.175	2.13	2.190	2.220	
840	.0009	.0095	.0010	.0016	2.175	2.13	2.190	2.220	
1224	.0007	.0067	.0012	.0016	2.175	2.13	2.190	2.220	
1320	.0007	.0067	.0015	.0019	2.175	2.13	2.190	2.220	
*1325	.027	.0160	.014	.0058	2.200	2.14	2.230	2.220	
1344	.057	.0280	.032	.0097	2.230	2.14	2.255	2.225	
1368	.072	.0390	.046	.0125	2.255	2.17	2.275	2.225	
1416	.053	.050	.069	.0145	2.245	2.18	2.300	2.230	
1488	.042	.063	.120	.0173	2.225	2.18	2.325	2.230	
1512	.042	.063	.120	.0180	2.215	2.19	2.365	2.235	
1560	.038	.061	.120	.0190	2.215	2.19	2.375	2.235	
1584	.038	.055	.120	.0195	2.210	2.18	2.380	2.240	
1656	.035	.043	.118	.020	2.195	2.17	2.335	2.240	
1728	.034	.040	.117	.020	2.190	2.15	2.325	2.235	
1752	.034	.039	.117	.020	2.190	2.14	2.305	2.235	
1824	.034	.037	.116	.020	2.190	2.14	2.305	2.230	
1848	.033	.036	.115	.0195	2.190	2.14	2.300	2.230	
1896	.026	.030	.093	.0180	2.180	2.13	2.290	2.230	

* - Recovery through 1320 hours in vacuum.
 1320 hours to 1848 hours in dry nitrogen at atmospheric pressure.
 1848 hours to 1896 hours in air.

Table 6. TFE-7 Vacuum X-Ray Exposure and Recovery Data, 1 kc.

Exposure Time (Hours)	Dissipation Factor				Dielectric Constant				Absorbed Dose (Mrads)
	A-2	N-2	A-16	N-16	A-2	N-2	A-16	N-16	
0	.0004	.0004	.0004	.0004	2.165	2.12	2.190	2.205	0
7	.0047	.0010	.0078	.0011	2.165	2.12	2.190	2.205	.18
23	.0084	.0010	.0048	.0017	2.165	2.12	2.190	2.205	.58
32	.0096	.0010	.0038	.0019	2.165	2.12	2.190	2.205	.80
47	.0090	.0011	.0026	.0022	2.165	2.12	2.190	2.205	1.18
73	.0082	.0013	.0018	.0028	2.165	2.12	2.190	2.205	1.83
85	.0059	.0015	.0015	.0029	2.165	2.12	2.190	2.205	2.13
168	.0038	.0036	.0010	.0028	2.165	2.12	2.190	2.205	4.22
192	.0032	.0042	.0010	.0028	2.165	2.12	2.190	2.205	4.83
215	.0031	.0047	.0010	.0028	2.165	2.12	2.190	2.210	5.40
242	.0030	.0051	.0010	.0029	2.165	2.12	2.190	2.210	6.08
266	.0030	.0052	.0009	.0030	2.165	2.12	2.190	2.210	6.67
336	.0030	.0052	.0008	.0030	2.165	2.12	2.190	2.210	8.44
360	.0029	.0051	.0008	.0029	2.165	2.13	2.190	2.210	9.03
384	.0027	.0050	.0008	.0027	2.165	2.13	2.190	2.210	9.64
408	.0024	.0045	.0008	.0025	2.165	2.13	2.190	2.210	10.2
503	.0017	.0041	.0008	.0018	2.165	2.13	2.190	2.210	12.6
552	.0017	.0040	.0008	.0018	2.165	2.13	2.190	2.210	13.8
597	.0016	.0039	.0008	.0018	2.165	2.13	2.190	2.210	15.0
668	.0009	.0038	.0008	.0018	2.165	2.13	2.190	2.210	16.7
Recovery									
Time (Hours)	Dissipation Factor				Dielectric Constant				Absorbed Dose (Mrads)
24	.0007	.0036	.0003	.0018	2.165	2.12	2.190	2.210	
72	.0007	.0034	.0003	.0014	2.165	2.12	2.190	2.210	
96	.0007	.0032	.0003	.0013	2.165	2.12	2.190	2.210	
168	.0008	.0029	.0003	.0011	2.165	2.12	2.190	2.210	
264	.0009	.0027	.0003	.0009	2.165	2.12	2.190	2.210	
360	.0012	.0027	.0003	.0008	2.165	2.12	2.190	2.210	
480	.0014	.0027	.0003	.0007	2.165	2.12	2.190	2.210	
840	.0015	.0018	.0003	.0006	2.165	2.12	2.190	2.210	
1224	.0011	.0011	.0009	.0007	2.165	2.12	2.190	2.210	
1320	.0010	.0010	.0009	.0008	2.165	2.12	2.190	2.210	
*1325	.0070	.0039	.0046	.0018	2.175	2.13	2.200	2.210	
1344	.0115	.0069	.0085	.0027	2.180	2.14	2.200	2.210	
1368	.0110	.0089	.0160	.0036	2.220	2.13	2.200	2.210	
1416	.0070	.0106	.0155	.0036	2.215	2.13	2.200	2.220	
1488	.0070	.0118	.0220	.0045	2.205	2.13	2.210	2.220	
1512	.0069	.0115	.0235	.0044	2.185	2.13	2.215	2.225	
1560	.0068	.0107	.0255	.0042	2.185	2.13	2.215	2.225	
1584	.0068	.0100	.0250	.0040	2.175	2.13	2.215	2.225	
1656	.0064	.0084	.0215	.0033	2.170	2.12	2.200	2.225	
1728	.0058	.0072	.0195	.0031	2.170	2.12	2.200	2.220	
1752	.0058	.0070	.0190	.0031	2.165	2.12	2.200	2.220	
1824	.0054	.0065	.0185	.0031	2.165	2.12	2.200	2.220	
1848	.0054	.0061	.0185	.0030	2.165	2.12	2.200	2.220	
1896	.0042	.0048	.0215	.0025	2.165	2.12	2.200	2.220	

* - Recovery through 1320 hours in vacuum.

1320 hours to 1848 hours in dry nitrogen at atmospheric pressure.

1848 hours to 1896 hours in air.

Table 7. TFE-7 Vacuum X-Ray Exposure and Recovery Data, 10 kc.

A-2 Sintered in air, 380°C, 2 hours.
 N-2 Sintered in nitrogen, 380°C, 2 hours.
 A-16 Sintered in air, 380°C, 16 hours.
 N-16 Sintered in nitrogen, 380°C, 16 hours.

Exposure Time (Hours)	Dissipation Factor				Dielectric Constant				Absorbed Dose (Mrads)
	A-2	N-2	A-16	N-16	A-2	N-2	A-16	N-16	
0	.0004	.0004	.0004	.0004	2.165	2.12	2.190	2.205	0
23	.0013	.0001	.0019	.0006	2.165	2.12	2.190	2.205	.58
32	.0016	.0001	.0015	.0007	2.165	2.12	2.190	2.205	.80
47	.0019	.0001	.0012	.0007	2.165	2.12	2.190	2.205	1.18
73	.0016	.0002	.0008	.0009	2.165	2.12	2.190	2.205	1.83
85	.0014	.0005	.0003	.0010	2.165	2.12	2.190	2.205	2.13
168	.0010	.0010	.0007	.0008	2.165	2.12	2.190	2.205	4.22
192	.0010	.0011	.0007	.0008	2.165	2.12	2.190	2.205	4.83
215	.0010	.0011	.0007	.0008	2.165	2.12	2.190	2.205	5.40
242	.0010	.0013	.0007	.0007	2.165	2.12	2.190	2.205	6.08
266	.0010	.0018	.0007	.0007	2.165	2.12	2.190	2.205	6.67
336	.0009	.0021	.0005	.0007	2.165	2.12	2.190	2.205	8.44
360	.0009	.0021	.0005	.0007	2.165	2.12	2.190	2.205	9.03
384	.0008	.0019	.0005	.0007	2.165	2.12	2.190	2.205	9.64
408	.0008	.0016	.0004	.0007	2.165	2.12	2.190	2.205	10.2
503	.0008	.0013	.0003	.0007	2.165	2.12	2.190	2.205	12.6
552	.0008	.0013	.0003	.0007	2.165	2.12	2.190	2.205	13.8
597	.0008	.0011	.0003	.0006	2.165	2.12	2.190	2.205	15.0
668	.0008	.0010	.0003	.0006	2.165	2.12	2.190	2.205	15.7
Recovery									
Time (Hours)									
24	.0007	.0010	.0003	.0005	2.165	2.12	2.190	2.205	
72	.0007	.0010	.0003	.0005	2.165	2.12	2.190	2.205	
96	.0007	.0010	.0003	.0005	2.165	2.12	2.190	2.205	
168	.0007	.0010	.0003	.0005	2.165	2.12	2.190	2.205	
264	.0005	.0009	.0003	.0005	2.165	2.12	2.190	2.205	
360	.0004	.0008	.0003	.0005	2.165	2.12	2.190	2.205	
480	.0004	.0006	.0003	.0005	2.165	2.12	2.190	2.205	
840	.0004	.0006	.0003	.0005	2.165	2.12	2.190	2.205	
1224	.0004	.0007	.0005	.0004	2.165	2.12	2.190	2.205	
1320	.0004	.0007	.0005	.0004	2.165	2.12	2.190	2.205	
*1325	.0014	.0015	.0010	.0005	2.170	2.12	2.190	2.205	
1344	.0019	.0016	.0017	.0006	2.175	2.13	2.190	2.205	
1368	.0020	.0021	.0018	.0008	2.175	2.13	2.190	2.205	
1416	.0020	.0021	.0016	.0011	2.175	2.13	2.190	2.210	
1488	.0015	.0019	.0015	.0012	2.170	2.13	2.195	2.210	
1512	.0014	.0018	.0015	.0011	2.170	2.13	2.195	2.210	
1560	.0013	.0017	.0014	.0010	2.170	2.13	2.195	2.210	
1584	.0012	.0016	.0014	.0009	2.170	2.13	2.195	2.210	
1656	.0011	.0013	.0013	.0006	2.165	2.13	2.190	2.210	
1728	.0011	.0013	.0012	.0005	2.165	2.13	2.190	2.205	
1752	.0011	.0013	.0012	.0005	2.165	2.13	2.190	2.205	
1824	.0011	.0012	.0012	.0004	2.165	2.13	2.190	2.205	
1848	.0011	.0012	.0012	.0004	2.165	2.13	2.190	2.205	
1896	.0006	.0010	.0010	.0004	2.165	2.13	2.190	2.205	

* - Recovery through 1320 hours in vacuum.
 1320 hours to 1848 hours in dry nitrogen at atmospheric pressure.
 1848 hours to 1896 hours in air.

Table 8. TFE-7 Vacuum X-Ray Exposure and Recovery Data, 100 kc.

Exposure Time (Hours)	Dissipation Factor				Dielectric Constant				Absorbed Dose (Mrads)
	A-2	N-2	A-16	N-16	A-2	N-2	A-16	N-16	
0	.0004	.0004	.0004	.0004	2.165	2.12	2.185	2.205	0
23	.0011	.0008	.0011	.0004	2.165	2.12	2.185	2.205	.58
32	.0010	.0007	.0009	.0002	2.165	2.12	2.185	2.205	.80
47	.0008	.0007	.0006	.0002	2.165	2.12	2.185	2.205	1.18
73	.0007	.0007	.0005	.0002	2.165	2.12	2.185	2.205	1.83
85	.0007	.0007	.0005	.0002	2.165	2.12	2.185	2.205	2.13
168	.0007	.0008	.0005	.0004	2.165	2.12	2.185	2.205	4.22
192	.0007	.0008	.0005	.0005	2.165	2.12	2.185	2.205	4.83
215	.0007	.0008	.0005	.0006	2.165	2.12	2.185	2.205	5.40
242	.0007	.0008	.0005	.0007	2.165	2.12	2.185	2.205	6.08
266	.0007	.0008	.0005	.0007	2.165	2.12	2.185	2.205	6.67
336	.0005	.0008	.0004	.0007	2.165	2.12	2.185	2.205	8.44
360	.0005	.0008	.0004	.0007	2.165	2.12	2.185	2.205	9.03
384	.0005	.0008	.0004	.0007	2.165	2.12	2.185	2.205	9.64
408	.0005	.0008	.0004	.0007	2.165	2.12	2.185	2.205	10.2
503	.0005	.0008	.0004	.0007	2.165	2.12	2.185	2.205	12.6
552	.0005	.0008	.0004	.0007	2.165	2.12	2.185	2.205	13.8
597	.0005	.0008	.0004	.0007	2.165	2.12	2.185	2.205	15.0
668	.0005	.0008	.0004	.0007	2.165	2.12	2.185	2.205	16.7
Recovery Time (Hours)									
24	.0005	.0008	.0004	.0007	2.165	2.12	2.185	2.205	
72	.0005	.0008	.0004	.0007	2.165	2.12	2.185	2.205	
96	.0005	.0008	.0004	.0007	2.165	2.12	2.185	2.205	
168	.0005	.0008	.0004	.0007	2.165	2.12	2.185	2.205	
264	.0005	.0008	.0004	.0007	2.165	2.12	2.185	2.205	
360	.0005	.0007	.0004	.0007	2.165	2.12	2.185	2.205	
480	.0005	.0006	.0004	.0007	2.165	2.12	2.185	2.205	
840	.0005	.0006	.0004	.0007	2.165	2.12	2.185	2.205	
1224	.0005	.0006	.0004	.0007	2.165	2.12	2.185	2.205	
1320	.0005	.0006	.0004	.0007	2.165	2.12	2.185	2.205	
*1325	.0011	.0009	.0009	.0008	2.170	2.12	2.185	2.205	
1344	.0012	.0012	.0010	.0008	2.175	2.13	2.185	2.205	
1368	.0013	.0015	.0012	.0008	2.175	2.13	2.185	2.205	
1416	.0013	.0015	.0011	.0008	2.175	2.12	2.185	2.210	
1488	.0012	.0013	.0011	.0008	2.170	2.12	2.190	2.210	
1512	.0011	.0012	.0010	.0008	2.170	2.12	2.190	2.210	
1560	.0011	.0012	.0010	.0008	2.170	2.12	2.190	2.210	
1584	.0010	.0012	.0010	.0008	2.170	2.12	2.190	2.210	
1656	.0010	.0011	.0009	.0007	2.165	2.12	2.190	2.210	
1728	.0010	.0011	.0009	.0007	2.165	2.12	2.190	2.205	
1752	.0009	.0010	.0009	.0007	2.165	2.12	2.190	2.205	
1824	.0009	.0010	.0008	.0007	2.165	2.12	2.190	2.205	
1848	.0009	.0010	.0008	.0007	2.165	2.12	2.190	2.205	
1896	.0006	.0009	.0007	.0007	2.165	2.12	2.190	2.205	

* - Recovery through 1320 hours in vacuum.
 1320 hours to 1848 hours in dry nitrogen at atmospheric pressure.
 1848 hours to 1896 hours in air.

X. Illustrations.

<u>Figure</u>	<u>Description</u>	<u>Page</u>
1	Test cell for vacuum sparkover measurements in presence of magnetic field.	53
2	Specimen/electrode system for x-ray induced conductivity measurements in high vacuum.	54
3	Effect of voltage on x-ray induced conductivity. Dose rate 550 rads/min (H ₂ O).	55
4	Effect of absorbed dose on x-ray induced conductivity of Mylar-C.	56
5	Effect of dose rate on σ_m .	57
6	Effect of temperature on σ_x for Mylar-C.	58
7	Pressure change in vacuum chamber during x-ray irradiation of Mylar-C.	59
8	Effect of x-ray exposure on TFE-6; previous data.	60
9	Recovery characteristics of TFE-6; previous data.	61
10	Effect of absorbed dose on 100 cps $\tan\delta$ of TFE-7; 30-mil machined and 125-mil machined specimens from 1/2" thick block, 30-mil film skived from large diameter cylinder.	62
11	100 cps $\tan\delta$ recovery characteristics of TFE-7 after exposure shown in Figure 10.	63
12	Effect of absorbed dose on 100 cps dielectric constant of TFE-7; 30-mil and 125-mil machined specimens from 1/2" thick block, 30-mil film skived from large cylinder.	64
13	100 cps dielectric constant recovery characteristics after exposure shown in Figure 12.	65

<u>Figure</u>	<u>Description</u>	<u>Page</u>
14	Effect of sintering conditions on x-ray induced $\tan\delta$ of TFE-7 at 100 cps.	66
15	Effect of sintering on 100 cps $\tan\delta$ recovery characteristics of TFE-7 after exposure shown in Figure 14.	67
16	Effect of sintering on x-ray induced change in 100 cps dielectric constant of TFE-7.	68
17	Effect of sintering on 100 cps dielectric constant recovery characteristics of TFE-7 after exposure shown in Figure 16.	69
18	Cross-sectional view of specimen for electric strength measurements at frequencies up to 100 Mc.	70

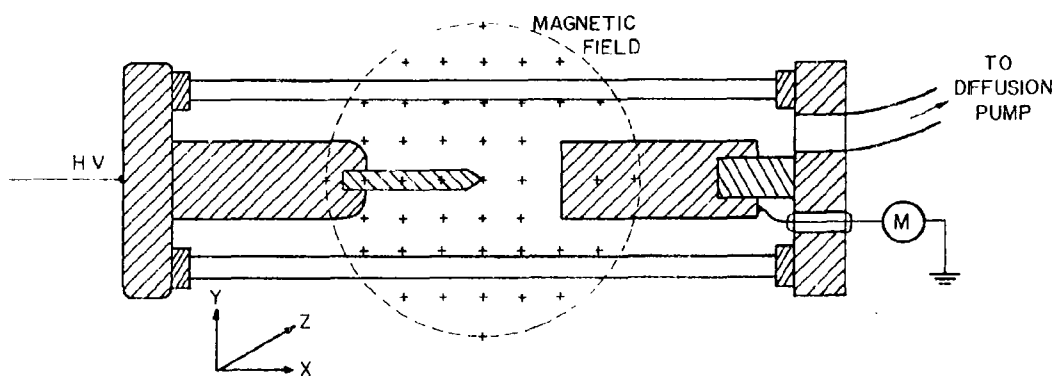


Figure 1. Test cell for vacuum sparkover measurements in presence of magnetic field. Pointed cathode, plane anode.

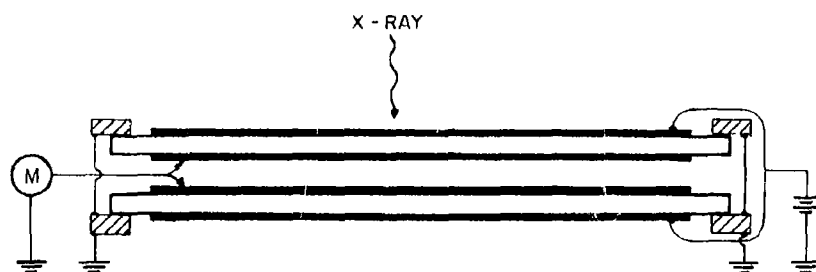


Figure 2. Specimen/electrode system for x-ray induced conductivity measurements in high vacuum.

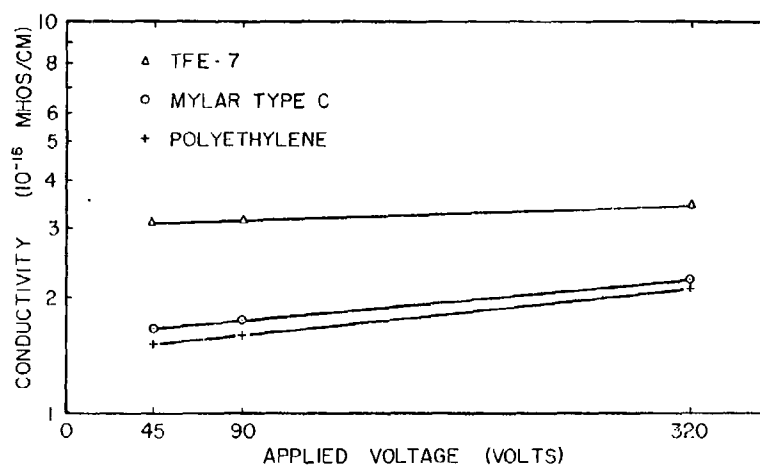


Figure 3. Effect of voltage on x-ray induced conductivity. Dose rate 550 rads/min (H_2O).

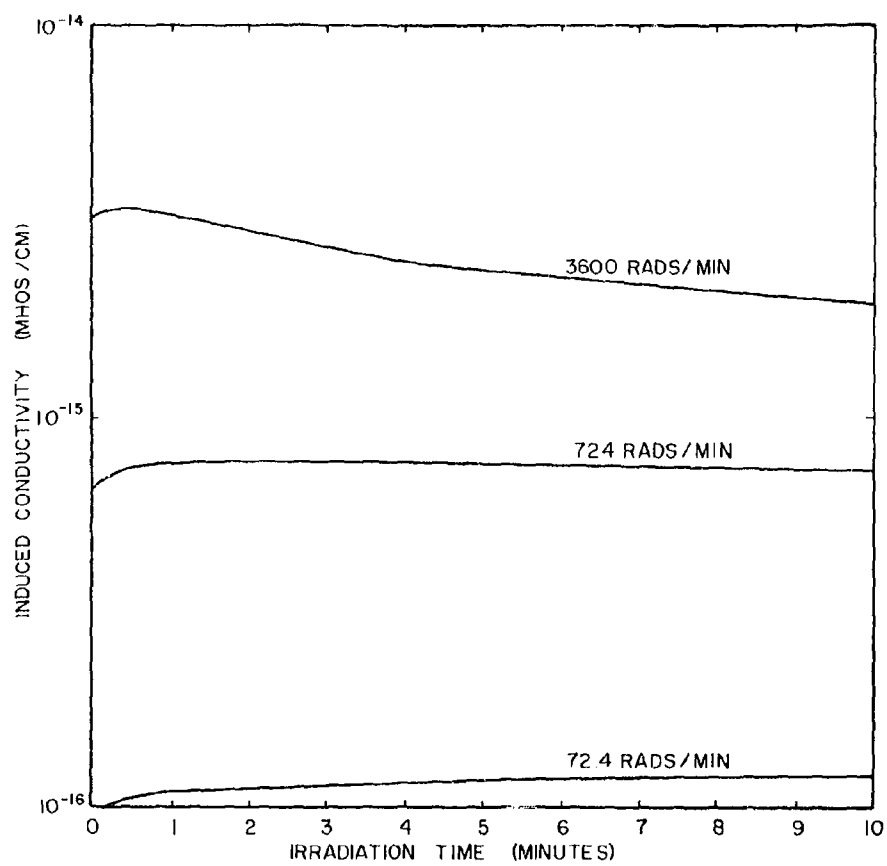
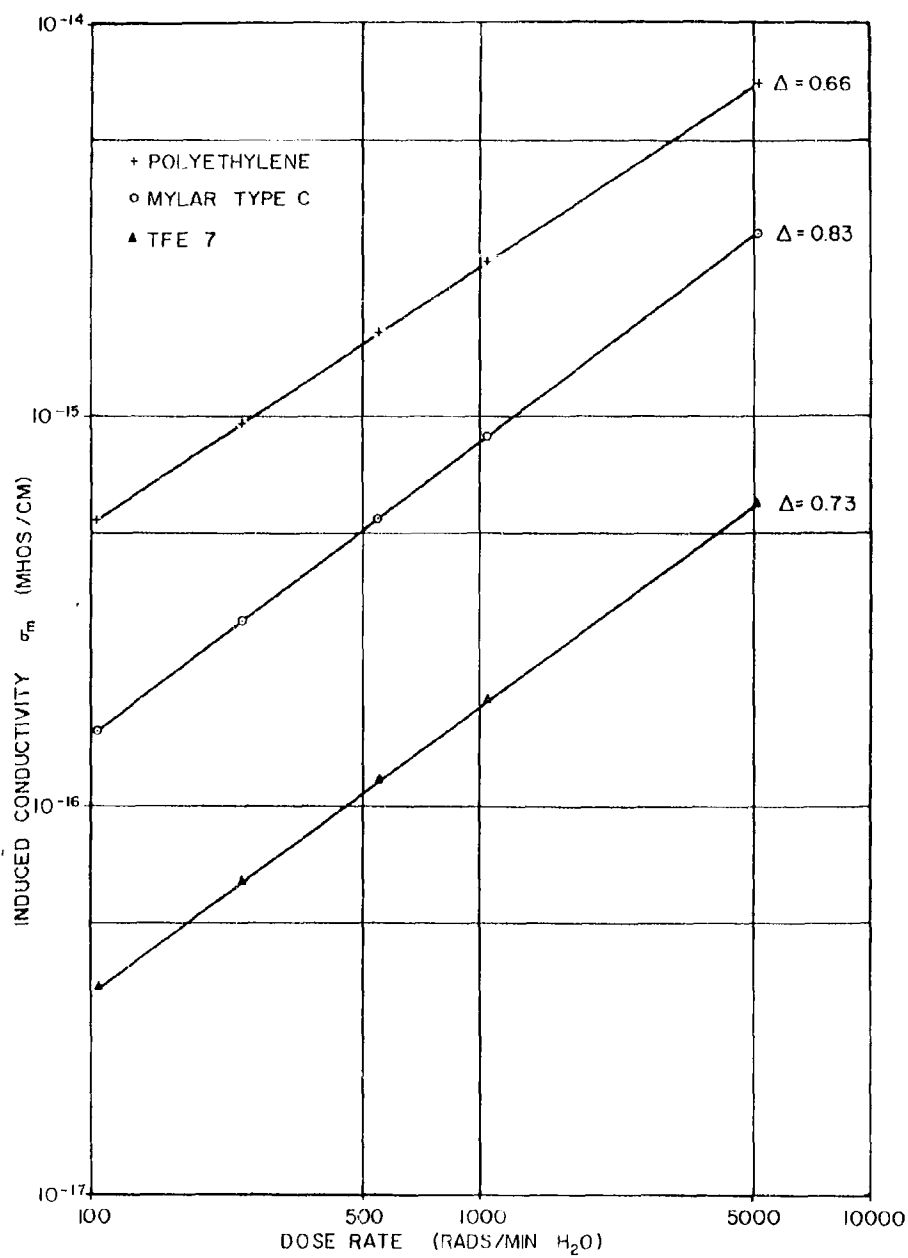


Figure 4. Effect of absorbed dose on x-ray induced conductivity of Mylar-C.

Figure 5. Effect of dose rate on σ_m .

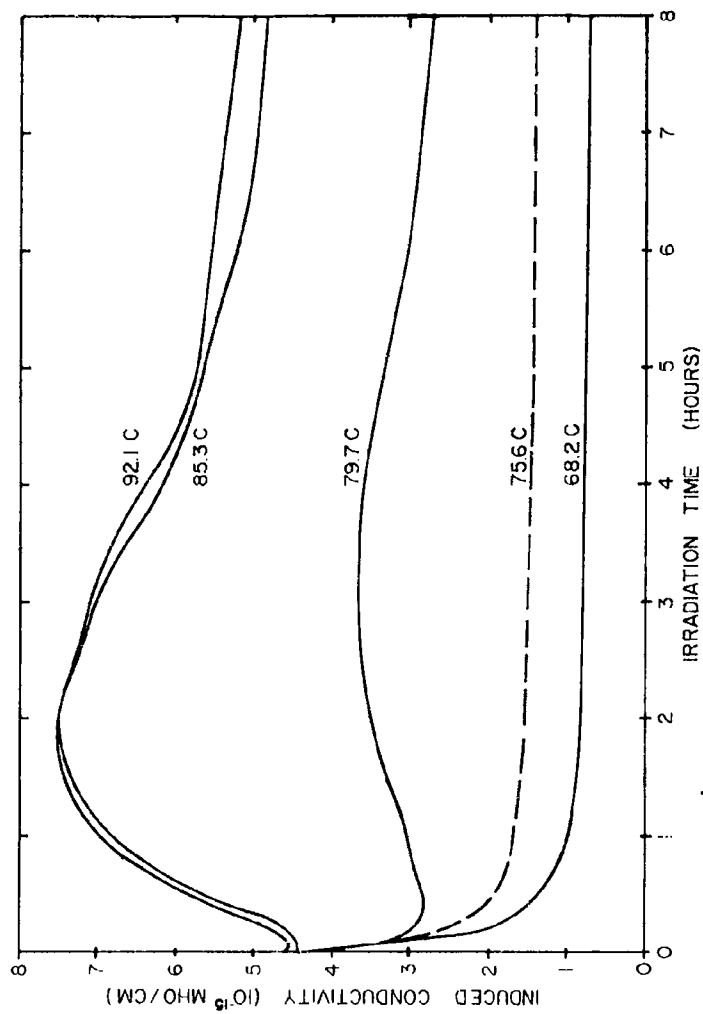


Figure 6. Effect of temperature on σ_x for Mylar-C. Dose rate 3400 rads/min. Corresponding pressure curves shown in Figure 7. Broken line indicates extra Mylar (100 sq.in.) in cell.

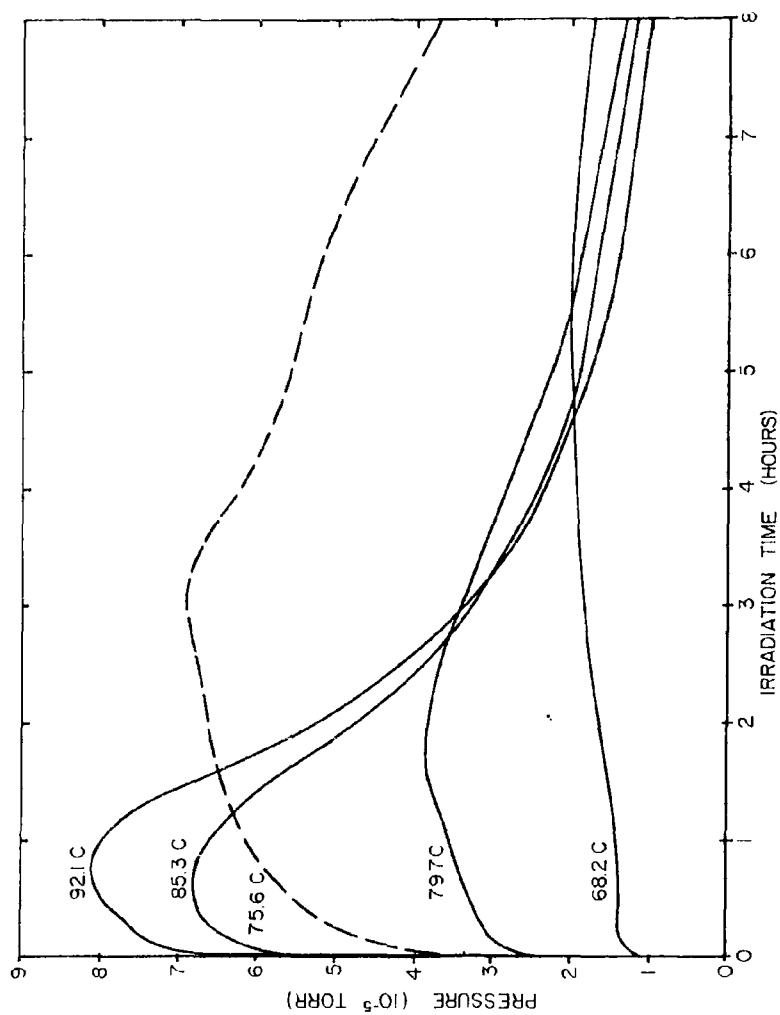


Figure 7. Pressure change in vacuum chamber during x-ray irradiation of Mylar-C. Broken line indicates extra Mylar (100 sq. in.) in cell.

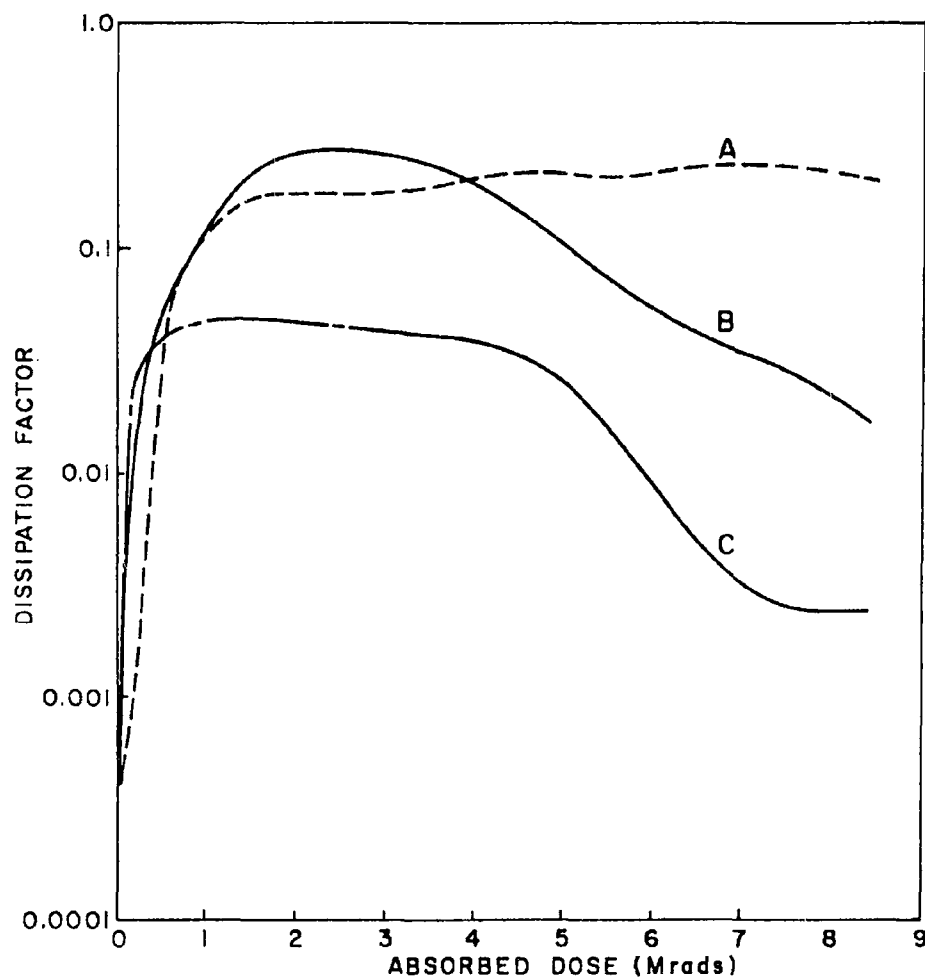


Figure 8. Effect of x-ray irradiation on TFE-6; previous data. Curve A - irradiated in air; Curve B - irradiated in vacuum; Curve C - irradiated in vacuum after previous dose of 8.5 megarads, followed by 10 months recovery in air.

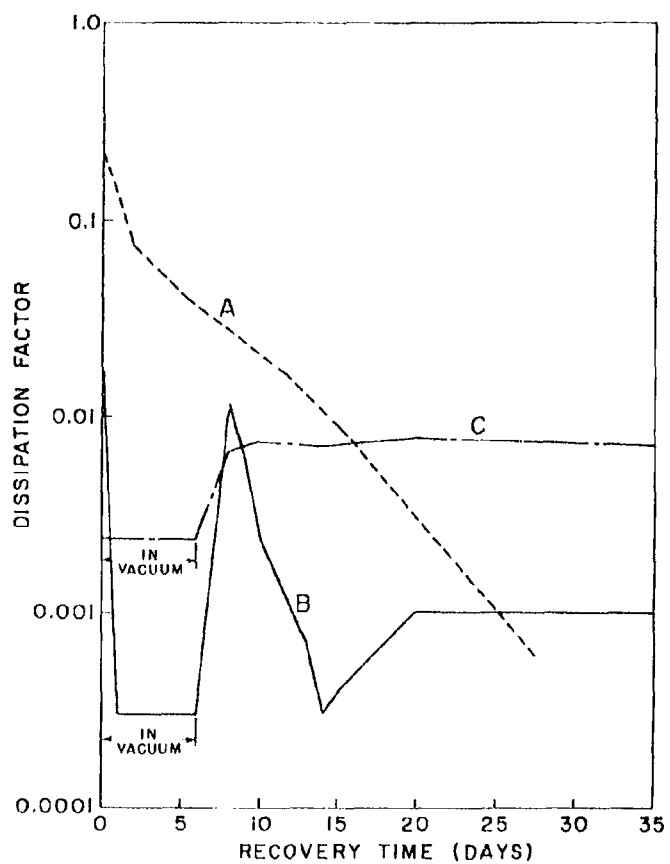


Figure 9. Recovery characteristics of TFE-6 specimens after x-ray irradiation as shown in Figure 8. Previous data.

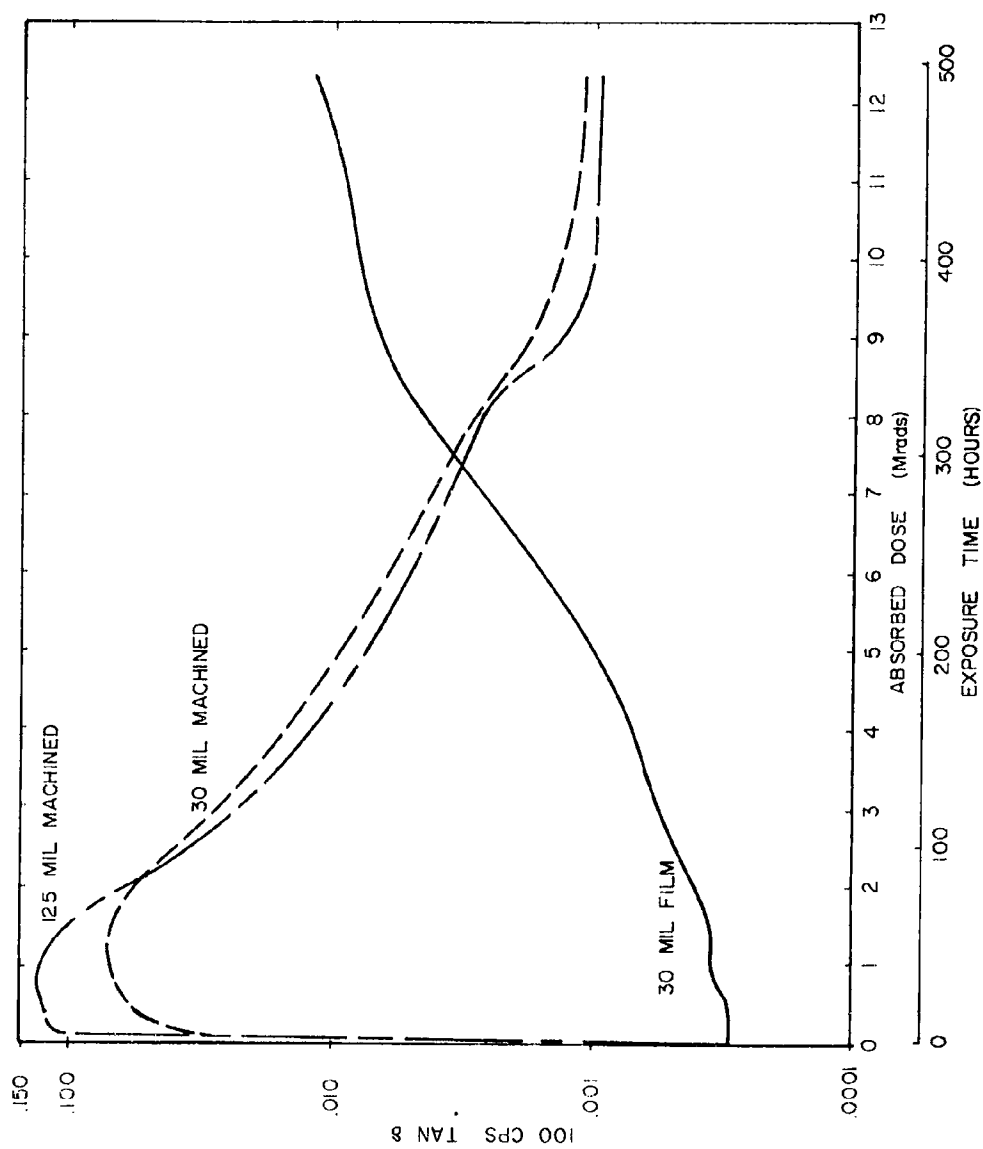


Figure 10. Effect of absorbed dose on 100 cps $\tan \delta$ of TFE-7; 30-mil machined and 125-mil machined specimens from 1/2" thick block, 30-mil film skived from large diameter cylinder.

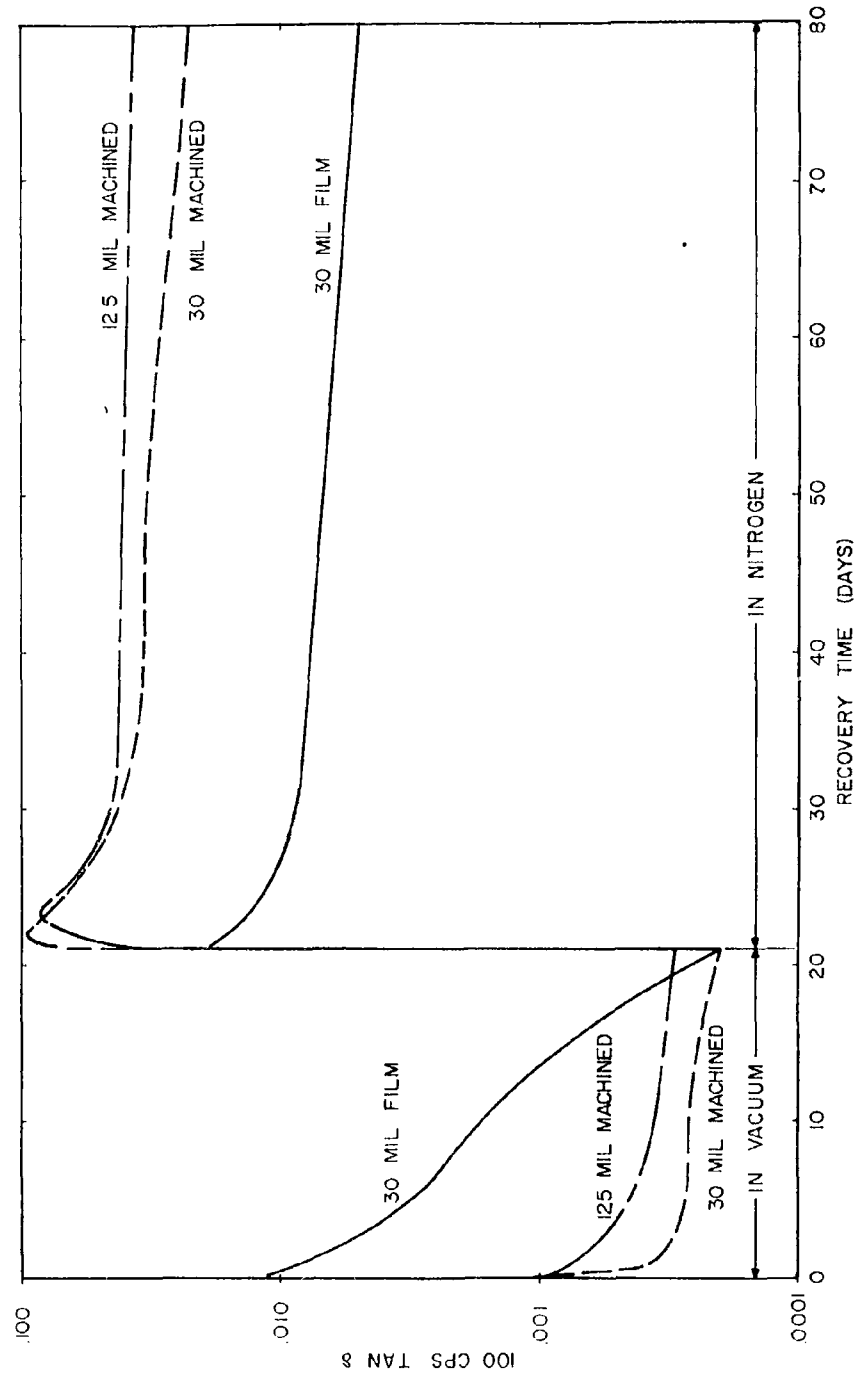


Figure 11. 100 cps $\tan \delta$ recovery characteristics of TFE-7 after exposure shown in Figure 10.

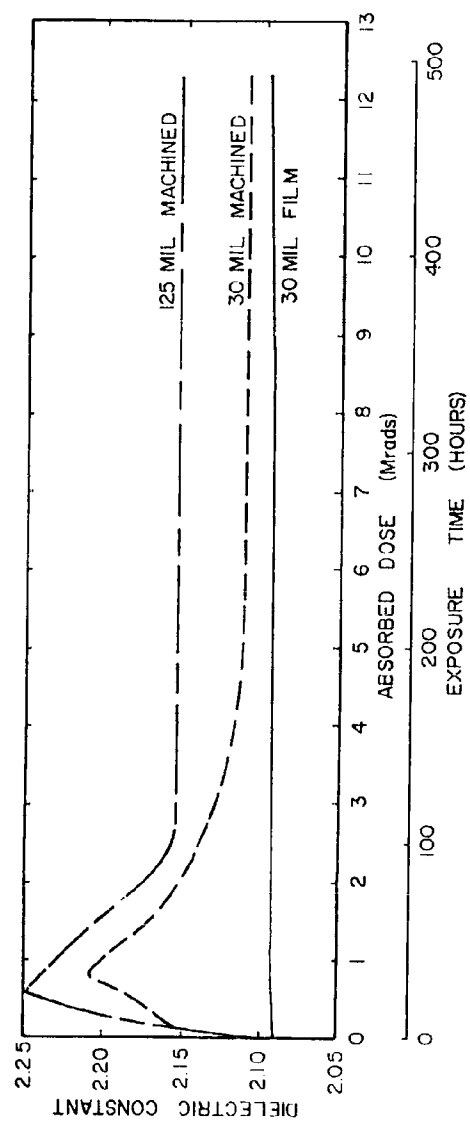


Figure 12. Effect of absorbed dose on 100 cps dielectric constant of TFE-7; 30-mil and 125-mil machined specimens from 1/2" thick block, 30-mil film skived from large cylinder.

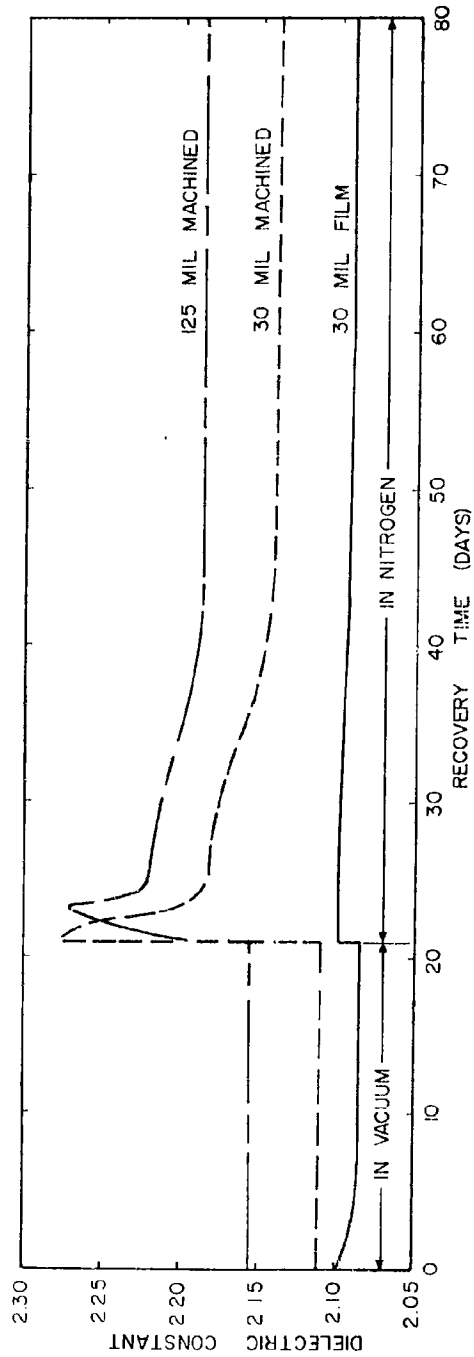


Figure 13. 100 cps dielectric constant recovery characteristics after exposure shown in Figure 12.

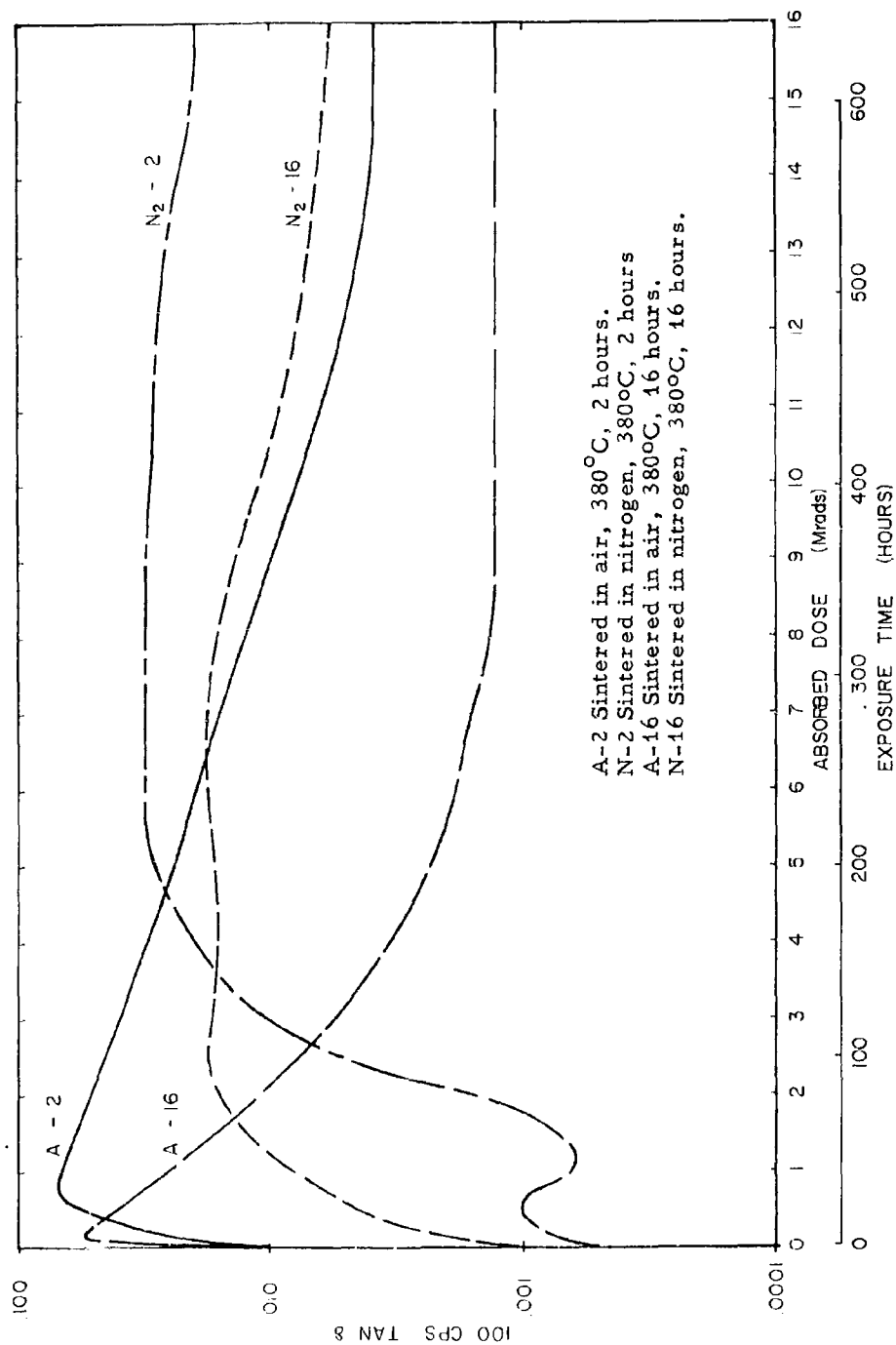


Figure 14. Effect of sintering conditions on x-ray induced $\tan \delta$ of TFE-7 at 100 cps.

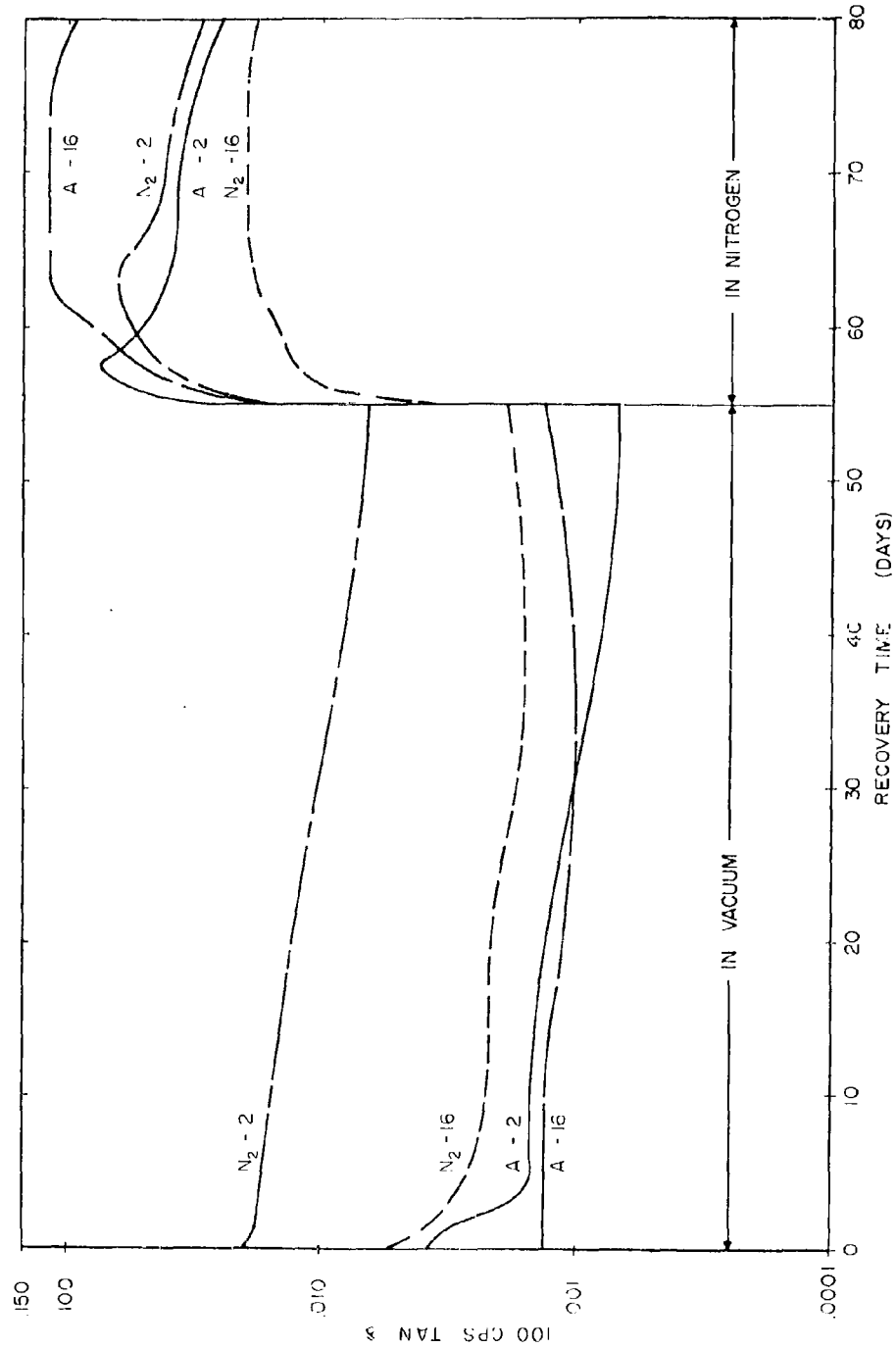


Figure 15. Effect of sintering on 10 cps $\tan \delta$ recovery characteristics of TFE-7 after exposure shown in Figure 14.

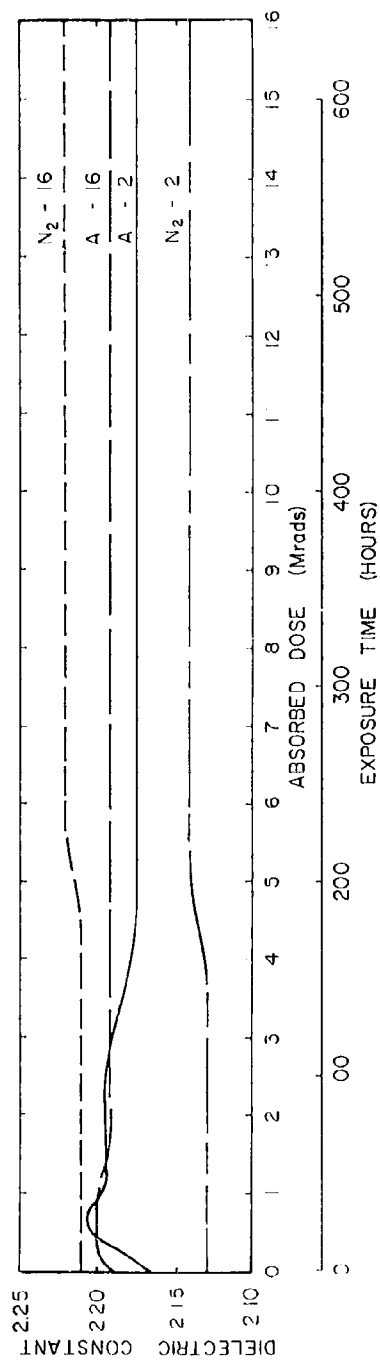
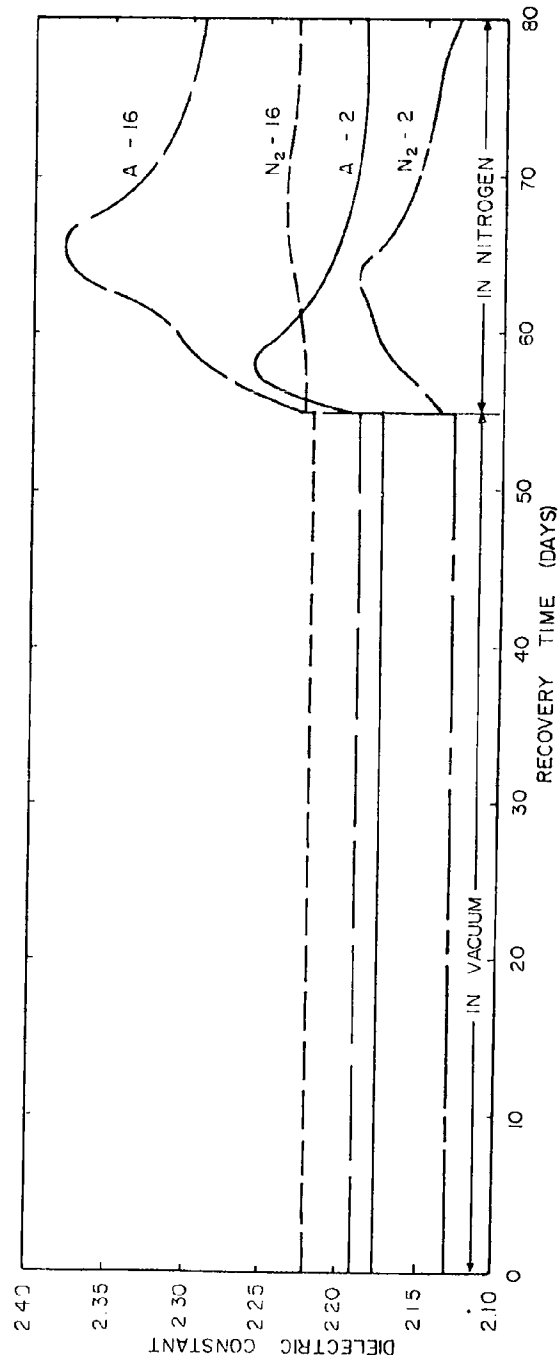


Figure 16. Effect of sintering on x-ray induced change in 100 cps dielectric constant of TFE-7. Sintered as shown in Figure 14.



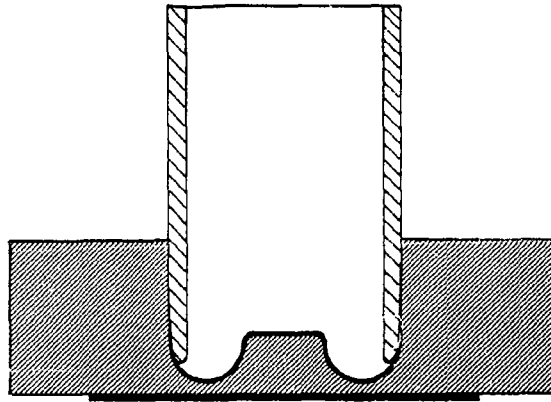


Figure 18. Cross-sectional view of specimen for electric strength measurements at frequencies up 100 Mc. Approximately twice full size.

Appendices:

- | | | |
|----------------|---|---------|
| Appendix I - | Summary of Tests on Multiconductor
Cable Connectors | Page-73 |
| Appendix II - | Summary of Electrical Data on
Siloxane Dielectric Compositions
for Antenna Mount Insulators | Page-87 |
| Appendix III - | Dielectric Properties of Extra-
terrestrial Dust | Page 97 |

The work summarized in these appendices was performed
at no additional cost to the Government.

APPENDIX I.

SUMMARY OF TESTS ON MULTICONDUCTOR CABLE CONNECTORS

1. Specimens.

Six cable connectors manufactured by the Bendix Scintilla Division, Sidney, New York were furnished by the Bendix Systems Division, Ann Arbor, Michigan. The connector parts were identified as follows:

SPOOCE-20-41S
SPO6CE-20-41P(SR)

Five connectors were wired and assembled by the Bendix Field Engineering Corporation, Baltimore, Maryland. The sixth connector was disassembled and the rubber insert was cut into sections to serve as weight-loss specimens.

A 6-inch length of wire (MIL 16878, 22AWG, Teflon Insulated) was connected to each pin, and the leads to pins A, C, E, G, J, L, N, R, T, V, Y, a, c, e, g, i, m, p, r and t were connected to a common high-voltage terminal. The remaining leads were connected to a common ground terminal either directly or through a Keithley Model 410 micromicroammeter, as described below.

2. Tests.

(a) Insulation Resistance.

Resistance measurements were made between the common terminals using a Keithley Model 410 micromicroammeter. Since alternate pins were connected to opposite terminals, these measurements indicate the overall insulation resistance of a mated connector.

(b) High-Voltage Performance.

The 60-cps corona starting voltages and breakdown voltages were determined by connecting one of the common terminals to a high-voltage lead while the other common terminal was grounded. The connector shell was connected to the grounded terminal. Corona was detected by inserting a 100 ohm resistor in the ground side of the circuit and monitoring the voltage across this resistor with an oscilloscope. The applied voltage was manually increased from zero to maximum in approximately 30-seconds.

Failures could occur between adjacent pins and between the connector shell and those pins that were connected to the high-voltage terminal.

3. Exploratory Measurements.

Since the number of specimens was so limited, several exploratory measurements were made on one mated connector, designated Specimen #1. Table I shows the measured values of resistance after a 5-minute electrification at each of several voltages in the range from 46 to 640 volts. At the end of 30-seconds of electrification, values were obtained that were within 10% of the values shown in Table I. Measurements made with reversed polarity yielded the same values of resistance. A voltage of 180 volts was selected for all subsequent measurements.

In a vacuum of approximately 1×10^{-5} torr, at room temperature the resistance of Specimen #1 increased from 7.12×10^9 to 1.56×10^{10} ohms after 64-hours of exposure. When the temperature of the connector was increased to 65°C the insulation resistance decreased rapidly to a minimum value of 2.88×10^7 ohms and then slowly increased during a 7-hour period to a value of 4.1×10^7 ohms. The detailed data are given in Table II. After cooling to room temperature, the cycle was repeated and these results are also given in Table II. It can be seen that the transient effect was moderated during the second run, but the overall behavior was similar to that observed during the first exposure. In both cases the heater was turned on at zero time and an equilibrium temperature of about 65°C was reached after 30-minutes.

After 24-hours of exposure at 65°C in the vacuum chamber, x-ray irradiation was introduced. The data are given in Table III, where it can be seen that the gradual increase in resistance that had been evident before the introduction of x-rays, continued during the 150-hour exposure period. This indicates that the irradiation had no significant effect on the insulation resistance.

At the end of the 150-hour exposure period, the voltage was increased to 640-volts and the insulation resistance was the same as that measured at 180-volts.

A 60-cps high-voltage test was then conducted, using a 100 ohm resistor on the grounded side to provide a signal which could be monitored with an oscilloscope to determine the corona starting voltage. Corona was detected at an applied voltage of 1000 volts rms and a breakdown occurred after two minutes of voltage application. The connector was removed from the cell and opened for inspection. The breakdown had occurred at the interface of the connector insulators between pins N and P, where N had been connected to the high-voltage. The leads to these pins were removed

from the common terminals and the connector was again placed in the vacuum chamber. After 39-hours at 65°C the insulation resistance was the same as it had been at the end of the previous run.

A second high-voltage test again resulted in corona at about 1000 volts rms. A breakdown occurred between pins L and M, where L was connected to the high-voltage. Arcing also occurred between K and L but a complete track was not formed.

These exploratory measurements provided the information required to set up a long-time test on the four remaining specimens.

4. Long-Time Tests.

Specimens 2, 3, 4 and 5 were placed in the vacuum chamber in a horizontal position, one above the other, with their axes in a plane perpendicular to the x-ray beam and approximately 44 cm from the x-ray target. From top to bottom the order was 2, 3, 4, 5. In each case pin L was closest to the front of the chamber, toward the beam. The sliced rubber insulator segments were hung on bare hook-up wire just above connector #2. Thermocouples were attached to each connector shell and one was placed approximately 1/8-inch in front of the connectors between specimens 2 and 3. A thermistor used in the thermostatic control circuit was also placed at this same location. An incandescent lamp which served as a heat source was located at the front of the cell, approximately 20 cm from the specimens.

The x-ray generator utilizes a Machlett AEG-50 tube with a tungsten target operating at 50 KV peak, 50 ma. The equivalent carbon dose rate in the plane of the specimens was about 0.1 megarads per hour.

The chamber was pumped down over a 64-hour period to reduce the amount of outgassing that was expected when the temperature was increased. In spite of this long initial pump-down period,

when the specimens were heated the pressure increased from 1×10^{-5} torr to 1×10^{-4} torr and did not drop to 5×10^{-5} torr until 7-hours of heating had elapsed.

After one hour of heating, Specimen #5 was tested for 60-cps corona starting voltage, which was determined to be 1200 volts rms.

The insulation resistance data obtained during a 344-hour exposure period are given in Table IV. The minimum values occurred at approximately 1 1/2-hours after heating began. The average temperature of the group of connectors was $63 \pm 2^{\circ}\text{C}$, while each connector temperature was maintained constant within 1°C .

Slight temperature fluctuations proved to be important during the period when the insulation resistance was slowly increasing. It appeared that the temperature coefficient of resistance was -10 to -15% per degree Centigrade in the temperature range near 65°C .

It will be noted that after 344-hours the insulation resistance in each case is about two decades lower than the room temperature value and increasing very slowly. As mentioned previously, this behavior is caused by the temperature increase rather than the x-ray irradiation.

The 60-cps corona starting voltage was measured at 344-hours for each connector. In all cases corona was detected at about 700 volts rms and complete breakdown occurred at about 2500 volts rms. Table V indicates the location of the complete and partial failures for each connector. It should be mentioned that a sustained voltage of 700 volts caused detectable corona but did not lead to a complete breakdown after several minutes. It was necessary to increase the applied voltage to obtain a breakdown.

After the high-voltage tests were completed, the cell was opened and the connectors were inspected. In each case it was difficult to uncouple the mated connectors because of adhesion of the rubber insulator in one body to its counterpart in the other body.

Weight measurements were made on one rubber insert that had been sliced into three pieces. This insert consists of two parts which are bonded to form a single piece. The insert that separates the pins is a black rubber, while the opposite end that separates the wires is a brown rubber which has a wax-like feel. The three weight-loss specimens are identified as black, transition and brown to indicate the section of the insert from which they were taken. Table VI shows the percentage loss in weight after the 344-hour exposure and at various intervals during subsequent storage at laboratory condition. The nominal weights of the three specimens were: black 10 gms, transition 3 gms, and brown 7 gms.

The data show that both materials exhibit significant weight losses which are only slightly affected by storage at laboratory condition for 24-hours.

The data of Table VI show that both rubber compositions exhibit significant weight loss after 344-hours in high-vacuum. Slight increases in weight were observed during a 24-hour recovery period at laboratory condition. This weight recovery, which occurs with many materials, is usually associated with moisture absorption.

All three specimens were much stiffer after exposure and the brown material had become darkened in the areas that had been directly exposed to the x-ray beam. The inserts in the connectors, which were shielded from the x-rays by the connector shells, did not become as stiff as the specimens that were directly exposed. Consequently, additional tests would be required to determine the extent to which the irradiation affected the physical properties.

5. Conclusions.

Exposure to high-vacuum and x-ray irradiation did not cause any serious changes in the electrical performance of the connectors, but physical changes in the rubber insert were observed. The largest

change in overall insulation resistance was caused by increased temperature, rather than reduced pressure or irradiation.

Longer exposure times would be required to determine if the weight loss and stiffening of the rubber insert would lead to mechanical failure. It appears that the life of the connector in a space environment would be determined by mechanical rather than electrical properties.

Table I. Specimen #1, Insulation Resistance at 25°C,
Atmospheric Pressure.

<u>Volts</u>	<u>Ohms</u>
45	7.50×10^9
90	7.44×10^9
135	7.18×10^9
180	7.12×10^9
320	7.12×10^9
640	7.08×10^9

Table II. Specimen #1, Effect on Exposure at 65°C, 10⁻⁵ torr
On Insulation Resistance.

<u>Exposure Time</u> <u>(Hours)</u>	<u>1st cycle</u> <u>(ohms)</u>	<u>2nd cycle</u> <u>(ohms)</u>
0	1.56x10 ¹⁰	1.33x10 ¹⁰
0.5*	1.17x10 ⁸	9.22x10 ⁷
1.0	3.53x10 ⁷	4.68x10 ⁷
1.5	2.98x10 ⁷	3.96x10 ⁷
2.0	2.88x10 ⁷	3.96x10 ⁷
2.5	2.93x10 ⁷	4.19x10 ⁷
3.0	3.00x10 ⁷	4.50x10 ⁷
3.5	3.16x10 ⁷	4.74x10 ⁷
4.0	3.19x10 ⁷	4.87x10 ⁷
4.5	3.30x10 ⁷	5.14x10 ⁷
5.0	3.39x10 ⁷	5.45x10 ⁷
5.5	3.64x10 ⁷	5.63x10 ⁷
6.0	3.83x10 ⁷	5.81x10 ⁷
6.5	4.00x10 ⁷	6.00x10 ⁷
7.0	4.18x10 ⁷	6.41x10 ⁷
7.5		6.72x10 ⁷
22.0		1.15x10 ⁸

* Heating started at zero time; temperature constant at 65°C after 0.5 hours.

Table III. Specimen #1, Effect of Exposure to X-Ray Irradiation
at 65°C, 10⁻⁵ torr on Insulation Resistance.

Exposure Time (Hours)	Resistance (ohms)	Exposure Time (Hours)	Resistance (ohms)
0	1.17x10 ⁸	74.5	3.02x10 ⁸
0.5	1.15x10 ⁸	75.0	3.05x10 ⁸
1.0	1.12x10 ⁸	77.0	2.90x10 ⁸
1.5	1.09x10 ⁸	78.0	2.84x10 ⁸
2.0	1.11x10 ⁸	79.0	2.91x10 ⁸
2.5	1.11x10 ⁸	95.5	3.53x10 ⁸
3.0	1.11x10 ⁸	96.5	3.21x10 ⁸
3.5	1.14x10 ⁸	97.0	3.08x10 ⁸
4.0	1.15x10 ⁸	98.0	2.97x10 ⁸
4.5	1.15x10 ⁸	99.0	2.97x10 ⁸
5.0	1.17x10 ⁸	100	2.98x10 ⁸
5.5	1.18x10 ⁸	101	3.00x10 ⁸
6.0	1.19x10 ⁸	102	3.02x10 ⁸
6.5	1.22x10 ⁸	103	3.11x10 ⁸
7.0	1.24x10 ⁸	104	3.18x10 ⁸
7.5	1.25x10 ⁸	120	3.66x10 ⁸
8.0	1.29x10 ⁸	121	3.56x10 ⁸
8.5	1.33x10 ⁸	122	3.39x10 ⁸
23.5	1.78x10 ⁸	123	3.40x10 ⁸
24.0	1.78x10 ⁸	125	3.59x10 ⁸
25.0	1.67x10 ⁸	126	3.61x10 ⁸
26.0	1.64x10 ⁸	127	3.52x10 ⁸
29.0	1.72x10 ⁸	128	3.54x10 ⁸
31.0	1.78x10 ⁸	143	4.10x10 ⁸
32.0	1.80x10 ⁸	144	3.91x10 ⁸
47.5	2.33x10 ⁸	145	3.84x10 ⁸
49.0	2.15x10 ⁸	146	3.69x10 ⁸
50.0	2.14x10 ⁸	147	3.66x10 ⁸
51.0	2.14x10 ⁸	148	4.00x10 ⁸
52.0	2.21x10 ⁸	150	4.09x10 ⁸
53.0	2.21x10 ⁸		
55.0	2.39x10 ⁸		

Table IV. Effect of Exposure to X-Ray Irradiation at 65°C,
10⁻⁵ torr on Insulation Resistance.

Exposure Time (Hours)	Insulation Resistance (ohms)			
	Spec. 2	Spec. 3	Spec. 4	Spec. 5
0	2.81x10 ¹⁰	3.05x10 ¹⁰	3.34x10 ¹⁰	3.58x10 ¹⁰
0.5	1.44x10 ⁸	1.11x10 ⁸	1.62x10 ⁸	4.45x10 ⁸
1.0	3.37x10 ⁷	2.75x10 ⁷	3.53x10 ⁷	6.25x10 ⁷
1.5	2.25x10 ⁷	1.90x10 ⁷	2.27x10 ⁷	3.83x10 ⁷
2.0	2.54x10 ⁷	2.16x10 ⁷	2.52x10 ⁷	4.09x10 ⁷
2.5	2.56x10 ⁷	2.20x10 ⁷	2.27x10 ⁷	4.09x10 ⁷
3.0	2.65x10 ⁷	2.31x10 ⁷	2.61x10 ⁷	4.09x10 ⁷
3.5	2.73x10 ⁷	2.42x10 ⁷	2.71x10 ⁷	4.00x10 ⁷
4.0	2.79x10 ⁷	2.49x10 ⁷	2.79x10 ⁷	4.05x10 ⁷
4.5	2.95x10 ⁷	2.67x10 ⁷	2.95x10 ⁷	4.14x10 ⁷
5.0	3.11x10 ⁷	2.84x10 ⁷	3.08x10 ⁷	4.39x10 ⁷
6.0	3.60x10 ⁷	3.36x10 ⁷	3.64x10 ⁷	4.87x10 ⁷
7.0	3.87x10 ⁷	3.67x10 ⁷	3.96x10 ⁷	5.22x10 ⁷
8.0	4.18x10 ⁷	4.05x10 ⁷	4.34x10 ⁷	5.63x10 ⁷
24.0	8.78x10 ⁷	8.78x10 ⁷	9.62x10 ⁷	1.21x10 ⁸
26.0	8.66x10 ⁷	8.66x10 ⁷	9.37x10 ⁷	1.18x10 ⁸
28.0	9.10x10 ⁷	9.00x10 ⁷	9.83x10 ⁷	1.22x10 ⁸
30.0	9.33x10 ⁷	9.23x10 ⁷	1.01x10 ⁸	1.26x10 ⁸
33.0	1.03x10 ⁸	1.02x10 ⁸	1.12x10 ⁸	1.41x10 ⁸
48.0	1.59x10 ⁸	1.56x10 ⁸	1.75x10 ⁸	2.16x10 ⁸
56.0	1.67x10 ⁸	1.62x10 ⁸	1.80x10 ⁸	2.24x10 ⁸
72.0	1.85x10 ⁸	1.78x10 ⁸	1.96x10 ⁸	2.59x10 ⁸
78.0	1.90x10 ⁸	1.78x10 ⁸	1.98x10 ⁸	2.65x10 ⁸
96.0	2.50x10 ⁸	2.29x10 ⁸	2.61x10 ⁸	3.54x10 ⁸
104	2.59x10 ⁸	2.38x10 ⁸	2.71x10 ⁸	3.65x10 ⁸
168	3.92x10 ⁸	3.47x10 ⁸	4.09x10 ⁸	5.72x10 ⁸
192	4.28x10 ⁸	3.83x10 ⁸	4.50x10 ⁸	6.43x10 ⁸
200	4.28x10 ⁸	3.75x10 ⁸	4.39x10 ⁸	6.33x10 ⁸
220	3.83x10 ⁸	3.34x10 ⁸	4.00x10 ⁸	5.72x10 ⁸
240	4.18x10 ⁸	3.71x10 ⁸	4.48x10 ⁸	6.43x10 ⁸
248	4.14x10 ⁸	3.62x10 ⁸	4.39x10 ⁸	6.37x10 ⁸
264	4.47x10 ⁸	3.91x10 ⁸	4.73x10 ⁸	6.97x10 ⁸
272	4.38x10 ⁸	3.82x10 ⁸	4.66x10 ⁸	6.69x10 ⁸
344	5.14x10 ⁸	4.56x10 ⁸	5.46x10 ⁸	8.07x10 ⁸

Table V. Failure Locations. Tracks formed on flat surface of rubber insert between pin locations shown.

<u>Specimen</u>	<u>Complete Track</u>		<u>Partial Track</u>	
	<u>High</u>	<u>Ground</u>	<u>High</u>	<u>Ground</u>
1	N L	P M	L	K
2	C	B		
3	T	S	C	D
4	J	M		
5	A	B	L N	M M

Table VI. Percentage weight loss of rubber insert sections after exposure to x-ray irradiation at 65°C, 10⁻⁵ torr for 344-hours.

Time elapsed after removal from chamber (hours)	Black Specimen	Transition Specimen	Brown Specimen
0	3.224	5.405	6.114
0.5	3.204	5.362	6.088
1	3.200	5.353	6.081
2	3.192	5.334	6.065
3	3.189	5.328	6.060
4	3.184	5.320	6.053
5	3.180	5.312	6.047
7	3.175	5.304	6.038
24	3.143	5.237	5.982

APPENDIX II.

SUMMARY OF ELECTRICAL DATA ON SILOXANE DIELECTRIC
COMPOSITIONS FOR ANTENNA-MOUNT INSULATORS

In a report submitted to USAERDL on May 9, 1962, test results on several antenna-mount insulators and insulating materials were presented. Among the materials included in that study were two siloxane compositions (C-1928 and C-1941) supplied by the Delaware Research and Development Corporation, Wilmington, Delaware. To provide further information on materials of this type, additional measurements have been made on several siloxane compositions and are reported herein.

The material designated C-1977 in this report is the same composition type as the materials designated C-1928 and C-1941 in the previous report. This material was used in the fabrication of antenna-mount insulators tested in the previous study.

All specimens used in this series of tests were provided by the Delaware Research and Development Corporation on a no-cost basis.

The test methods employed in all measurements have been described in numerous reports issued by the Dielectrics Laboratory. Tables I and II include loss data at frequencies other than those normally used at this laboratory. These values were obtained at several other laboratories and compiled by the Delaware Research and Development Corporation.

Flashover and electric strength tests were made by applying a gradually increasing voltage from zero to maximum in approximately 40-seconds. Flashover tests at 100% RH were made on specimens that were mounted in a conditioning chamber and left undisturbed until after the measurements were completed. Condensation on the surfaces of the specimens and the electrodes contributes to the spread in results.

Table I. Summary of Dielectric Constant Data on Siloxane
Compositions. *

<u>Frequency</u>	<u>C-1977</u>	<u>C-1928</u>	<u>C-1147</u>	<u>C-1994</u>	<u>C-1983</u>	<u>C-1985</u>	<u>C-1989</u>
60 cps	2.375	2.39					
100 cps	2.375						
1 Kc	2.367	2.39					
10 Kc	2.350	2.38	2.50				
100 Kc	2.346		2.52				
2 Mc	2.335	2.38	2.51	5.63	5.94	9.04	2.57
18 Mc	2.310	2.24					
40 Mc	2.282						
100 Mc	2.240	2.20	2.49				
250 Mc			2.51				
300 Mc	2.26						
1 Gc	2.255		2.50		5.99		
3 Gc	2.26		2.50		6.04		
8.5 Gc	2.266		2.49	5.77	6.10		2.64
9.2 Gc					6.02		
9.375 Gc			2.51			9.19	
14 Gc			2.48				

* Includes data from other laboratories compiled by Delaware Research and Development Corporation.

Table II. Summary of Dissipation Factor Data on Siloxane Compositions, *

<u>Frequency</u>	<u>C-1977</u>	<u>C-1928</u>	<u>C-1147</u>	<u>C-1994</u>	<u>C-1983</u>	<u>C-1985</u>	<u>C-1989</u>
60 cps	.00128	<.0005					
100 cps	.00159						
1 Kc	.00191	<.0005					
10 Kc	.00137	<.0005	.0002				
100 Kc	.00137		.0001				
2 Mc	.00067	.0003	.0002	.0012	.0014	.0021	.0006
18 Mc	.00083	.0006					
40 Mc	.00079						
100 Mc	.00061	.0018	.0002				
250 Mc			.0003				
300 Mc	.00099						
1 Gc	.00103		.0004		.0018		
3 Gc	.00104		.0006		.0034		
8.5 Gc	.00148		.0007	.0042	.0039		.0012
9.2 Gc					.0040		
9.375 Gc			.0008			.0023	
14 Gc			.0009				

* Includes data from other laboratories compiled by Delaware Research and Development Corporation.

Table III. Effect of Temperature and Moisture Absorption on Loss Properties of Composition C-1928.(1)

<u>Condition</u>	<u>ϵ'</u>	<u>$\tan \delta$</u>
25C/100%RH	2.39	L ⁽²⁾

85C-1 hour	2.32	L
85C-24 hours	2.34	L
After 1 hour recovery	2.37	L

25C/100%RH, 1 hour	2.39	L
25C/100%RH-24 hours	2.40	.005
After 1 hour recovery	2.39	L

(1) Average values for two specimens.

(2) L = Less than 0.0005.

Table IV. Effect of Exposure at 30°C, 100% RH on D-C Surface
Resistivity (ohms per square). One minute electrification.

<u>Exposure Time (Hours)</u>	<u>C-1977</u>	<u>C-1994</u>	<u>C-1983</u>	<u>C-1995</u>
Initial	4.5×10^{17}	1.3×10^{15}	2.1×10^{14}	2.3×10^{17}
24	1.2×10^{12}	9.0×10^{10}	1.0×10^{12}	1.2×10^{10}
48	1.3×10^{13}	2.1×10^{10}	1.5×10^{11}	1.2×10^{10}
72	8.0×10^{12}			
88		3.3×10^9	3.5×10^{10}	1.3×10^{10}
96	1.4×10^{13}	9.0×10^9	5.8×10^{10}	2.4×10^{10}
<u>Recovery⁽¹⁾ Time (Hours)</u>				
1	3.1×10^{17}	4.2×10^{11}	3.4×10^{12}	5.0×10^{16}
24		3.3×10^{13}	3.4×10^{13}	2.9×10^{17}
64	1.0×10^{18}			

(1) Recovery at 50%RH.

Table V. Effect of Exposure at 30°C, 100% RH on D-C Volume Resistivity (ohm-cm). One minute electrification.

<u>Exposure Time (Hours)</u>	<u>C-1977</u>	<u>C-1994</u>	<u>C-1983</u>	<u>C-1995</u>
Initial	1.4×10^{18}	2.6×10^{14}	1.0×10^{14}	1.2×10^{17}
24	1.7×10^{13}	1.5×10^{13}	1.5×10^{12}	5.6×10^{13}
48	1.1×10^{13}	3.8×10^{12}	8.3×10^{12}	3.7×10^{12}
72	1.3×10^{13}			
88		1.0×10^{13}	4.0×10^{12}	3.0×10^{12}
96	1.2×10^{13}	8.0×10^{12}	3.1×10^{12}	7.1×10^{12}
Recovery ⁽¹⁾				
<u>Time (Hours)</u>				
1	2.7×10^{17}	1.4×10^{13}	2.2×10^{12}	1.1×10^{17}
24				
64	4.3×10^{17}	9.0×10^{12}	9.0×10^{12}	1.8×10^{17}

(1) Recovery at 50%RH.

Table VI. Average Values of Electric Strength (rms VPM);
Recessed Electrodes, 1/2" Diameter Tapered
Electrode.

<u>Composition</u>	<u>60 cps</u>			<u>2 Mc</u>			<u>18 Mc</u>		
	<u>No. Tests</u>	<u>Mils</u>	<u>VPM</u>	<u>No. Tests</u>	<u>Mils</u>	<u>VPM</u>	<u>No. Tests</u>	<u>Mils</u>	<u>VPM</u>
C-1977	4	40	1044	3	33	375	3	33	144
C-1977 after 24 hours at 30C/100RH	4	33	1480	3	32	335	4	35	108
C-1147	4	43	1175	4	45	509	4	42	214
C-1994	6	41	980	4	47	147	4	45	59*
C-1983	3	42	986	2	42	163	2	46	54*
C-1985	8	44	411	4	45	96#	3	45	37*
C-1989	16	40	815	8	45	206	10	45	60*

* Thermal failure.

Puncture accompanied by significant heating.

Table VII. Flashover Voltage (rms KV), 3/4" Diameter Electrodes,
3/8" Gap. Initial Values and Exposure Data at 30°C,
100% RH with Condensation.

<u>Composition</u>	<u>Exposure Time (hours)</u>	<u>60 cps</u>		<u>2 Mc</u>		<u>18 Mc</u>	
		<u>No. Tests</u>	<u>KV</u>	<u>No. Tests</u>	<u>KV</u>	<u>No. Tests</u>	<u>KV</u>
C-1977	Initial	4	13.8 ⁽¹⁾	4	12.3	3	10.8
	1	3	9.3	4	10.9		
	24	5	8.2	4	8.5		
C-1447	Initial			4	10.6	4	10.5
	96			4	7.7	4	8.0
C-1994	Initial	3	9.3	3	8.0	3	6.5
	1	2	9.4	1	5.5		
	24	4	9.4	1	4.2		
C-1983	Initial	3	9.0	3	6.5	3	6.0
	1	3	8.4	1	6.0		
	24	3	8.5	1	3.7		
C-1985	Initial	3	7.8				
	1	3	7.9				
C-1989	Initial	6	11.8	3	11.0	3	7.7
	1	5	8.3	3	8.7		
	24	3	8.0	3	8.0		

(1) 1st Rerun same specimens - 14.1 KV
2nd Rerun same specimens - 14.3 KV

APPENDIX III.

DIELECTRIC PROPERTIES OF EXTRATERRESTRIAL DUST

Measurements of dielectric constant and dissipation factor were made on specimens of extraterrestrial sediment from ice melters located at the South Pole Station. Specimens identified as Material I and Material II were prepared at USAERDL, Fort Monmouth, New Jersey in the following way:

Material I. Passed through 40 mesh screen.

Material II. Passed through 40 mesh screen and heated at 600°C for one hour to burn off organic contaminants.

A small cell was made which permitted the powdered material to be poured into the space between a pair of parallel plate electrodes. The electrodes were 3" x 3" and were separated by a distance of 1/8". This cell was used for measurements over the frequency range of 750 kc to 20 Mc. The measurements were made with a Boonton Model 260-A Q-Meter.

Preliminary measurements were made on: (a) the loose material, immediately after it was poured into the cell; (b) the settled material, after standing for one hour, and (c) the compact material. The compact specimen was formed by vibrating the cell until the volume of material no longer decreased. No differences could be detected between the loose and the settled specimens, so no further measurements were made on the settled material.

A smaller cell with shorter leads was required for measurements with a Boonton Model 190-A Q-Meter in the frequency range of 100 to 200 Mc. An existing sample holder was modified for this purpose. It was necessary to insert a polystyrene ring between the electrodes to maintain a fixed separation. The volume of material

between the electrodes was 1.765" in diameter and 0.137" thick. It was not possible to make measurements on the loose material with this cell.

Measurements were made on both materials in the as-received condition and after being dried at 50°C for 90-hours. Density determinations were made each time a cell was loaded. All measurements were made at room temperature.

The results are summarized in Table I. It should be noted that the densities for the 100 to 200 Mc specimens were significantly lower than the compact specimens obtained in the larger cell. Consequently, the high-frequency data is more in line with the low-frequency measurements on the loose material.

The importance of residual moisture content is demonstrated by the significantly lower $\tan\delta$ of the dried specimens of Material II. A further reduction in $\tan\delta$ would probably be observed if the measurements were made on specimens that were placed in a high-vacuum chamber.

To make meaningful measurements in the 1.0 to 8.6 kmc range it would have been necessary to modify the available Dielectrometer. It was not possible to load the powdered material in the waveguide and accurately determine the position of the specimen surface. With such a low dielectric constant material it would be necessary to fill the waveguide to a depth of about 2-inches and to determine this depth with an accuracy of a few mils. Even if a known weight of powder could be poured into the guide, the variation in packing would be great enough to introduce a prohibitive error in the calculated depth.

Table I. Dielectric Constant and Dissipation Factor of
Extraterrestrial Dust from the South Pole Station.

<u>Material I</u>		<u>750 KC</u>	<u>1 Mc</u>	<u>10 Mc</u>	<u>15 Mc</u>	<u>20 Mc</u>	<u>Density</u> <u>(gm/cm³)</u>
As-received Loose	ϵ'	2.28	2.24	2.24	2.17	2.09	0.459
	$\tan\delta$	0.045	0.047	0.045	0.042	0.056	
As-received Compact	ϵ'	3.22	3.14	2.99	2.91	2.78	0.620
	$\tan\delta$	0.050	0.048	0.053	0.051	0.066	
Dried Loose	ϵ'	2.25	2.19	2.19	2.11	2.02	0.445
	$\tan\delta$	0.043	0.042	0.048	0.042	0.058	
Dried Compact	ϵ'	3.24	3.04	2.92	2.84	2.69	0.614
	$\tan\delta$	0.047	0.044	0.047	0.046	0.062	
<u>Material II</u>							
As-received Loose	ϵ'	1.39	1.85	1.73	1.72	1.69	0.496
	$\tan\delta$	0.207	0.167	0.058	0.044	0.053	
As-received Compact	ϵ'	2.46	2.40	2.24	2.11	2.06	0.685
	$\tan\delta$	0.213	0.193	0.058	0.047	0.056	
Dried Loose	ϵ'	1.77	1.76	1.75	1.69	1.61	0.503
	$\tan\delta$	0.055	0.047	0.018	0.022	0.023	
Dried Compact	ϵ'	2.22	2.22	2.17	2.11	2.04	0.707
	$\tan\delta$	0.081	0.059	0.077	0.024	0.025	

<u>Material I</u>		<u>100 Mc</u>	<u>150 Mc</u>	<u>200 Mc</u>	<u>Density</u> <u>(gm/cm³)</u>
As-received Compact	ϵ'	1.50	1.35	1.25	0.464
	$\tan\delta$	0.054	0.050	0.064	
Dried Compact	ϵ'	1.53	1.36	1.25	0.573
	$\tan\delta$	0.056	0.054	0.046	
<u>Material II</u>					
As-received Compact	ϵ'	1.36	1.28	1.22	0.548
	$\tan\delta$	0.118	0.214	0.158	
Dried Compact	ϵ'	1.43	1.37	1.30	0.618
	$\tan\delta$	0.020	0.015	0.012	

Journal of Management Inquiry 18(6)
DOI: 10.1177/1056492609356106
© The Author(s) 2009
Reprints and permissions:
[sagepub.com/journalsPermissions.nav](http://www.sagepub.com/journalsPermissions.nav)

UNCLASSIFIED

UNCLASSIFIED

CLASSIFICATION:

120

[illegible][illegible]

234

2000

1. J. F. Fazio
2. A. W. Weinbaum
E. A. Symonakis
3. U.S. Army Electronics
Research and Development
Laboratory, Ft. Monmouth,
New Jersey
Contract DA-36-039-SC-8

25

6.
7.
8.
9.
10.

Director, Lab. John H. Egan, C. Entomologist and
 DIRECTOR FOR SALINITY AND SPACE VEHICLES by J. Egan, C. Entomologist and
 and a Symposium From Report 1967-1968, 1968, 1969, 1970, 1971, 1972, 1973, 1974, 1975, 1976, 1977, 1978, 1979, 1980, 1981, 1982, 1983, 1984, 1985, 1986, 1987, 1988, 1989, 1990, 1991, 1992, 1993, 1994, 1995, 1996, 1997, 1998, 1999, 2000, 2001, 2002, 2003, 2004, 2005, 2006, 2007, 2008, 2009, 2010, 2011, 2012, 2013, 2014, 2015, 2016, 2017, 2018, 2019, 2020, 2021, 2022, 2023, 2024, 2025, 2026, 2027, 2028, 2029, 2030, 2031, 2032, 2033, 2034, 2035, 2036, 2037, 2038, 2039, 2040, 2041, 2042, 2043, 2044, 2045, 2046, 2047, 2048, 2049, 2050, 2051, 2052, 2053, 2054, 2055, 2056, 2057, 2058, 2059, 2060, 2061, 2062, 2063, 2064, 2065, 2066, 2067, 2068, 2069, 2070, 2071, 2072, 2073, 2074, 2075, 2076, 2077, 2078, 2079, 2080, 2081, 2082, 2083, 2084, 2085, 2086, 2087, 2088, 2089, 2090, 2091, 2092, 2093, 2094, 2095, 2096, 2097, 2098, 2099, 2100, 2101, 2102, 2103, 2104, 2105, 2106, 2107, 2108, 2109, 2110, 2111, 2112, 2113, 2114, 2115, 2116, 2117, 2118, 2119, 2120, 2121, 2122, 2123, 2124, 2125, 2126, 2127, 2128, 2129, 2130, 2131, 2132, 2133, 2134, 2135, 2136, 2137, 2138, 2139, 2140, 2141, 2142, 2143, 2144, 2145, 2146, 2147, 2148, 2149, 2150, 2151, 2152, 2153, 2154, 2155, 2156, 2157, 2158, 2159, 2160, 2161, 2162, 2163, 2164, 2165, 2166, 2167, 2168, 2169, 2170, 2171, 2172, 2173, 2174, 2175, 2176, 2177, 2178, 2179, 2180, 2181, 2182, 2183, 2184, 2185, 2186, 2187, 2188, 2189, 2190, 2191, 2192, 2193, 2194, 2195, 2196, 2197, 2198, 2199, 2200, 2201, 2202, 2203, 2204, 2205, 2206, 2207, 2208, 2209, 2210, 2211, 2212, 2213, 2214, 2215, 2216, 2217, 2218, 2219, 2220, 2221, 2222, 2223, 2224, 2225, 2226, 2227, 2228, 2229, 2230, 2231, 2232, 2233, 2234, 2235, 2236, 2237, 2238, 2239, 2240, 2241, 2242, 2243, 2244, 2245, 2246, 2247, 2248, 2249, 2250, 2251, 2252, 2253, 2254, 2255, 2256, 2257, 2258, 2259, 2260, 2261, 2262, 2263, 2264, 2265, 2266, 2267, 2268, 2269, 2270, 2271, 2272, 2273, 2274, 2275, 2276, 2277, 2278, 2279, 2280, 2281, 2282, 2283, 2284, 2285, 2286, 2287, 2288, 2289, 2290, 2291, 2292, 2293, 2294, 2295, 2296, 2297, 2298, 2299, 2300, 2301, 2302, 2303, 2304, 2305, 2306, 2307, 2308, 2309, 2310, 2311, 2312, 2313, 2314, 2315, 2316, 2317, 2318, 2319, 2320, 2321, 2322, 2323, 2324, 2325, 2326, 2327, 2328, 2329, 2330, 2331, 2332, 2333, 2334, 2335, 2336, 2337, 2338, 2339, 2340, 2341, 2342, 2343, 2344, 2345, 2346, 2347, 2348, 2349, 2350, 2351, 2352, 2353, 2354, 2355, 2356, 2357, 2358, 2359, 2360, 2361, 2362, 2363, 2364, 2365, 2366, 2367, 2368, 2369, 2370, 2371, 2372, 2373, 2374, 2375, 2376, 2377, 2378, 2379, 2380, 2381, 2382, 2383, 2384, 2385, 2386, 2387, 2388, 2389, 2390, 2391, 2392, 2393, 2394, 2395, 2396, 2397, 2398, 2399, 2400, 2401, 2402, 2403, 2404, 2405, 2406, 2407, 2408, 2409, 2410, 2411, 2412, 2413, 2414, 2415, 2416, 2417, 2418, 2419, 2420, 2421, 2422, 2423, 2424, 2425, 2426, 2427, 2428, 2429, 2430, 2431, 2432, 2433, 2434, 2435, 2436, 2437, 2438, 2439, 2440, 2441, 2442, 2443, 2444, 2445, 2446, 2447, 2448, 2449, 2450, 2451, 2452, 2453, 2454, 2455, 2456, 2457, 2458, 2459, 2460, 2461, 2462, 2463, 2464, 2465, 2466, 2467, 2468, 2469, 2470, 2471, 2472, 2473, 2474, 2475, 2476, 2477, 2478, 2479, 2480, 2481, 2482, 2483, 2484, 2485, 2486, 2487, 2488, 2489, 2490, 2491, 2492, 2493, 2494, 2495, 2496, 2497, 2498, 2499, 2500, 2501, 2502, 2503, 2504, 2505, 2506, 2507, 2508, 2509, 2510, 2511, 2512, 2513, 2514, 2515, 2516, 2517, 2518, 2519, 2520, 2521, 2522, 2523, 2524, 2525, 2526, 2527, 2528, 2529, 2530, 2531, 2532, 2533, 2534, 2535, 2536, 2537, 2538, 2539, 2540, 2541, 2542, 2543, 2544, 2545, 2546, 2547, 2548, 2549, 2550, 2551, 2552, 2553, 2554, 2555, 2556, 2557, 2558, 2559, 2560, 2561, 2562, 2563, 2564, 2565, 2566, 2567, 2568, 2569, 2570, 2571, 2572, 2573, 2574, 2575, 2576, 2577, 2578, 2579, 2580, 2581, 2582, 2583, 2584, 2585, 2586, 2587, 2588, 2589, 2590, 2591, 2592, 2593, 2594, 2595, 2596, 2597, 2598, 2599, 2600, 2601, 2602, 2603, 2604, 2605, 2606, 2607, 2608, 2609, 2610, 2611, 2612, 2613, 2614, 2615, 2616, 2617, 2618, 2619, 2620, 2621, 2622, 2623, 2624, 2625, 2626, 2627, 2628, 2629, 2630, 2631, 2632, 2633, 2634, 2635, 2636, 2637, 2638, 2639

Geothermische Verfahren, Erdwärmepumpen, Solar-
thermische Erzeugung, Kälde, Vakuum-Eisungsmaschinen

Further results of a study of irradiated space environments on the properties of solid dielectric materials are reported.

As a result of the above, we have concluded that the effect of the above-mentioned factors on the rate of the reaction is not significant. The rate of the reaction is determined by the rate of the reaction of the reactants with the catalyst.

[illegible]

UNCLASSIFIED

X-ray induced a.c. losses in TFE resins (previously reported) are greatly influenced by the presence of oxygen during sintering. Diffusion (specimen thickness) plays a minor role in irradiation effects on a.c. loss properties.

An improved specimen for electric strength measurements on solids, at frequencies up to 100 Mc, is described.

Some phases of the investigation will be continued under Contract NAS8-5253.

UNCLASSIFIED

UNCLASSIFIED

X-ray induced a.c. losses in TFE resins (previously reported) are greatly influenced by the presence of oxygen during sintering. Diffusion (specimen thickness) plays a minor role in irradiation effects on a.c. loss properties.

An improved specimen for electric strength measurements on solids, at frequencies up to 100 Mc, is described.

Some phases of the investigation will be continued under Contract NAS8-5253.

UNCLASSIFIED

UNCLASSIFIED

X-ray induced a.c. losses in TFE resins (previously reported) are greatly influenced by the presence of oxygen during sintering. Diffusion (specimen thickness) plays a minor role in irradiation effects on a.c. loss properties.

An improved specimen for electric strength measurements on solids, at frequencies up to 100 Mc, is described.

Some phases of the investigation will be continued under Contract NAS8-5253.

UNCLASSIFIED

UNCLASSIFIED

X-ray induced a.c. losses in TFE resins (previously reported) are greatly influenced by the presence of oxygen during sintering. Diffusion (specimen thickness) plays a minor role in irradiation effects on a.c. loss properties.

An improved specimen for electric strength measurements on solids, at frequencies up to 100 Mc, is described.

Some phases of the investigation will be continued under Contract NAS8-5253.

UNCLASSIFIED

This Document
Reproduced From
Best Available Copy

DISTRIBUTION LIST

<u>No. of Copies</u>	<u>Destination</u>
1	- OASD (R&E), ATTN: Technical Library, Room 3E1065, The Pentagon, Washington 25, D.C.
1	- Chief of Research and Development, OCS, Department of the Army, Washington 25, D.C.
1	- Commanding General, U.S. Army Materiel Command, ATTN: R&D Directorate, Washington 25, D.C.
1	- Commanding General, U.S. Army Electronics Command, ATTN: AMSEL-AD, Fort Monmouth, New Jersey
1	- Director, U.S. Naval Research Laboratory, ATTN: Code 2027, Washington 25, D.C.
1	- Commander, Aeronautical Systems Division, ATTN: ASAPRL, Wright-Patterson Air Force Base, Ohio
1	- l'q., Electronic Systems Division, ATTN: ESAL, L.G. Hanscom Field, Bedford, Massachusetts
1	- Commander, Air Force Cambridge Research Laboratories, ATTN: CRO, L.G. Hanscom Field, Bedford, Massachusetts
1	- Commander, Air Force Command & Control Development Division, ATTN: CRZC, L.G. Hanscom Field, Bedford, Massachusetts
1	- Commander, Rome Air Development Center, ATTN: RAALD, Griffiss Air Force Base, New York
10	- Commander, Armed Services Technical Information Agency, ATTN: TISIA, Arlington Hall Station, Arlington 12, Virginia
2	- Chief, U.S. Army Security Agency, Arlington Hall Station, Arlington 12, Virginia
1	- Deputy President, U.S. Army Security Agency Board, Arlington Hall Station, Arlington 12, Virginia
1	- Commanding Officer, Harry Diamond Laboratories, ATTN: Library Room 211, Building 92, Washington 25, D.C.
1	- Corps of Engineers Liaison Office, U.S. Army Electronics Research and Development Laboratory, Fort Monmouth, New Jersey
1	- AFSC Scientific/Technical Liaison Office, U.S. Naval Air Development Center, Johnsville, Pennsylvania
1	- USAELRDL Liaison Office, Rome Air Development Center, ATTN: RAOL, Griffiss Air Force Base, New York
1	- Commanding Officer, U.S. Army Electronics Materiel Support Agency, ATTN: SELMS-ADJ, Fort Monmouth, New Jersey
1	- Marine Corps Liaison Office, U.S. Army Electronics Research and Development Laboratory, ATTN: SELRA/LNR, Fort Monmouth, New Jersey
1	- Commanding Officer, U.S. Army Electronics Research and Development Laboratory, ATTN: Director of Research or Engineering, Fort Monmouth, New Jersey
1	- Commanding Officer, U.S. Army Electronics Research and Development Laboratory, ATTN: Technical Documents Center, Fort Monmouth, New Jersey
1	- Commanding Officer, U.S. Army Electronics Research and Development Laboratory, ATTN: SELRA/ADJ (FU#1), Fort Monmouth, New Jersey
2	- Advisory Group on Electron Devices, 346 Broadway, New York 13, New York
3	- Commanding Officer, U.S. Army Electronics Research and Development Laboratory, ATTN: SELRA/TNR, Fort Monmouth, New Jersey (FOR RETRANSMITTAL TO ACCREDITED BRITISH AND CANADIAN GOVERNMENT REPRESENTATIVES)
1	- Commanding General, U.S. Army Combat Developments Command, ATTN: CDCMR-E, Fort Belvoir, Virginia
1	- Commanding Officer, U.S. Army Combat Developments Command, Communications-Electronics Agency, Fort Huachuca, Arizona
1	- Director, Fort Monmouth Office, U.S. Army Combat Developments Command, Communications-Electronics Agency, Building 410, Fort Monmouth, New Jersey
1	- AFSC Scientific/Technical Liaison Office, U.S. Army Electronics Research and Development Laboratory, Fort Monmouth, New Jersey
1	- Commanding Officer and Director, U.S. Navy Electronics Laboratory, San Diego 52, California
1	- E.I. du Pont de Nemours and Company, Inc., Plastics Department, ATTN: Mr. Joseph C. Reed, Wilmington, Delaware
1	- E.I. du Pont de Nemours and Company, Inc., Film Department, ATTN: Dr. Carl J. Heffelfinger, Circleville, Ohio
1	- Delaware Research and Development Corporation, ATTN: Mr. Charles L. Petze, 222 Sunset Drive, Wilmington, Delaware

**This Document
Reproduced From
Best Available Copy**

No. of
Copies

Destination

- 1 - Bendix Systems Division, ATTN: Mr. E. LaSalle, Ann Arbor, Michigan
- 1 - National Aeronautics and Space Administration, George C. Marshall Space Flight Center, ATTN: Mr. W.E. Bech, Huntsville, Alabama
- 1 - General Electric Company, ATTN: Dr. Robert S. Shane, Post Office Box 459, Utica, New York
- 1 - Lockheed Aircraft Corporation, Missiles & Space Division, ATTN: Dr. Francis J. Clauss (D/53-35) Sunnyvale, California
- 1 - Director, National Aeronautics & Space Agency, ATTN: O.R. Lloyd, Information Director, 1520 H Street, N.W., Washington 25, D.C.
- 1 - Picatinny Arsenal, Plastics Technical Evaluation Center, ATTN: H.E. Pebly, Jr., Director, Dover, New Jersey
- 1 - Commanding Officer, Quartermaster Research & Engineering Center, ATTN: QMREL-PRCN, Natick, Massachusetts
- 1 - Radio Corporation of America, Electron Tubes Division, ATTN: Mr. R.T. Jeffrey, Contract Administration, Harrison, New Jersey
- 1 - Bendix Corporation, Bendix Systems Division, ATTN: Mr. C.E. Jahnke, 3300 Plymouth Road, Ann Arbor, Michigan
- 1 - Director, National Aeronautics & Space Administration, Goddard Space Flight Center, ATTN: Mr. Aaron Fisher, Code 623, Greenbelt, Maryland
- 1 - Commanding General, U.S. Army Missile Command, ATTN: AMSMI-RGC, Redstone Arsenal, Alabama
- 1 - Commanding General, U.S. Army Satellite Communications Agency, Fort Monmouth, New Jersey
- 1 - Commanding Officer, U.S. A. Electronics Research & Development Laboratory, Fort Monmouth, New Jersey
- 1 - ATTN: SELRA/PE (Dr. E. Both)
- 1 - ATTN: SELRA/PE (Division Director)
- 16 - ATTN: SELRA/PEE (Mr. E. Linden)

**This Document
Reproduced From
Best Available Copy**